PHILOSOPHICAL TRANSACTIONS OF THE ROYAL SOCIETY A MATHEMATICAL, PHYSICAL & ENGINEERING SCIENCES

On the acoustics of an exponential boundary layer

L. M. B. C. Campos and P. G. T. A. SerrÃo

Phil. Trans. R. Soc. Lond. A 1998 **356**, 2335-2378
doi: 10.1098/rsta.1998.0277

THE ROYAL SOCIETY

On the acoustics of an exponential boundary layer

By L. M. B. C. Campos and P. G. T. A. Serrão

Secção de Mecânica Aeroespacial, ISR, Instituto Superior Técnico, 1096 Lisboa Codex, Portugal

Received 20 May 1996; accepted 9 December 1997

Contents

A brief derivation is given of the acoustic wave equation describing the propagation of sound in a unidirectional shear flow. This equation has been solved exactly in only one instance, namely a linear velocity profile; in the present paper a second exact solution is given, for the exponential velocity profile, which represents a boundary layer with weak suction at a high Reynolds number. The acoustic wave equation has a critical layer where the Doppler shifted frequency vanishes, and this corresponds to a regular singularity; another regular singularity corresponds to the free stream and the sound field consists either of propagating waves or of surface waves, showing that the critical layer can act as an absorbing layer. Analytical continuation is used to cover the whole flow region, from the wall boundary layer to the free stream; the appropriate boundary, radiation and stability conditions are discussed, and the acoustic pressure is plotted as a function of distance from the wall for several combinations of frequency, wavenumber parallel to the wall and low Mach number free-stream velocity; the combination of solutions appropriate to rigid and impedance walls is also plotted. The solutions are expressible in terms of Bessel functions only when the critical layer is in the free stream; when the critical layer is in the boundary layer, or when there is no critical layer, the solutions require an extension of the Gaussian hypergeometric equation, in which one of the three singularities is irregular; its solutions are extensions of Gaussian hypergeometric and Mathieu functions, whose general properties are discussed elsewhere.

Keywords: aeroacoustics; shear flow; sound propagation; refraction of sound; flow noise

1. Introduction

The propagation of sound in shear flows has been studied mostly by numerical and approximate analytical methods, with three motivations in mind: (i) propagation in ducts containing a shear flow (Pridmore-Brown 1958; Tack & Lambert 1965; Mungur & Gladwell 1969; Mungur & Plumblee 1969; Hersh & Catton 1971; Ko 1972; Eversman & Beckenmeyer 1972; Swinbanks 1975; Mani 1980; Ishii & Kakutani 1987); (ii) effect of boundary layers on sound near a wall (Shankar 1971, 1972*a*, *b*; Eversman 1971; Mariano 1971; Almgren 1976; Goldstein 1979, 1982; Myers & Chuang 1983; Hanson 1984); and (iii) effect of a laminar shear layer on sound transmission from a jet (Graham & Graham 1968; Balsa 1976*a*, *b*; Koutsoyannis *et al*. 1980). Concerning (ii) and (iii), besides the change in directivity due to laminar shear layers (Munt 1977) there is spectral broadening in turbulent flows (Lighthill 1953; Schmidt & Tilmann 1970; Ho & Kovasnay 1976; Campos 1978*a*, *b*, 1983*a*). There are no exact solutions of the acoustic wave equation in a turbulent flow, and even for a laminar unidirectional flow, only one exact solution has been published, namely for a linear velocity profile. In order for the velocity to remain bounded, the linear velocity profile is usually matched to a uniform velocity, to represent a boundary layer (Goldstein & Rice 1963; Scott 1979; Koutsoyannis 1980) on an infinite, or a semi-infinite (Jones 1978) plate, the latter involving an edge effect; the linear velocity profile has also been used to match two dissimilar uniform streams, providing a model of a 'simple' shear layer of finite thickness (Jones 1977), which is more sophisticated than the vortex sheet representation (Miles 1961). In the present paper a second exact solution of the acoustic wave equation in a unidirectional shear flow is given, for the case of an exponential velocity profile.

The acoustic wave equation has critical layers where the Doppler shifted frequency vanishes. There are many more instances of critical layers for waves in inhomogeneous and moving media, e.g. gravity (Booker & Bretherton 1966; Bretherton 1967; Turner 1973; Lighthill 1978), inertial (Greenspan 1968), hydromagnetic (McKenzie 1973; Eltayeb 1977; Campos 1983*b*, 1987*a*, 1988*a*, 1998) and instability (Lin 1955; Drazin & Reid 1981) waves; critical layers also occur in dissipative media at rest, e.g. for acoustic waves in the presence of viscosity (Yanowitch 1967; Campos 1983*c*), and thermal gradients and conduction (Lyons & Yanowitch 1974; Campos 1983*d*) and hydromagnetic waves in the presence of Ohmic electrical resistance (Campos 1983*c*, 1988*b*, 1990, 1993*a*, *b*) and Hall currents (McKenzie 1979; Campos & Isaeva 1992). Although some discussions of sound in shear flows do mention 'turning points' (e.g. Balsa 1976*a*, *b*), the existence of critical layers passes often unmentioned. For example, a linear velocity profile always has a critical layer, and if it is matched to a uniform stream, the critical layer will still exist if the Doppler shifted frequency is negative in the free stream. The same condition indicates whether a critical layer occurs for sound in an exponential shear flow. The main differences between the two cases are that (i) in a linear shear flow the vorticity is constant, and if it is matched to a uniform stream it jumps to zero across the matching point; and (ii) in an exponential shear flow the vorticity decays smoothly from the wall to the free stream.

In both cases there are two parameters in the velocity profile, allowing independent choice-free stream velocity and boundary layer thickness. The exponential shear flow is perhaps more realistic, in that it is an exact solution of the steady Navier–Stokes equation, with uniform wall suction, namely the asymptotic suction profile (Schlichting 1951). The suction becomes negligible at a high Reynolds number, i.e. for small viscosity; this is consistent with the neglect of viscosity, and other dissipative effects (e.g. thermal conduction) in the acoustic wave equation.

The present problem may also be considered from the point of view of stability of a shear flow (Lin 1955; Drazin & Reid 1981). The necessary conditions of stability of an inviscid incompressible shear flow are simple (Rayleigh 1880): any shear flow without inflection points is stable (e.g. the exponential). The stability criteria are less straightforward when generalizing to viscous incompressible shear flows. The instability waves, or Orr–Sommerfeld (Orr 1907; Sommerfeld 1908) waves in a viscous incompressible shear flow, become unstable beyond a critical Reynolds number, which signals the beginning of a complex process of transition to turbulence (Schlichting 1951). There are few exact solutions to the Orr–Sommerfeld equation in its original, or simplified Tollmien–Schlichting (Tollmien 1929; Schlichting 1933), forms. Both of these linear wave equations, describing the small amplitude disturbances of an incompressible viscous flow, are of the fourth order; neglecting viscosity leads to a second-order equation for the stability of an incompressible shear flow, known as Rayleigh's equation (Rayleigh 1880). The present paper considers inviscid but compressible perturbations. Thus the same fundamental wave equation specifies (i) the propagation of non-dissipative sound waves of small amplitude in a shear flow; and (ii) the linear stability of an inviscid compressible shear flow. The method of solution of the wave equation is different: (i) the stability is best approached by an initial value problem, e.g. as for a linear shear flow (Jones 1977, 1978); (ii) the sound propagation can be approached as a boundary-value problem, with eigenvalues and eigenfunctions in a finite domain like a duct (Mohring *et al*. 1983), or a continuous spectrum in a semi-infinite domain like a wall boundary layer (present case). The sound propagation and compressible stability problems are related, not only mathematically but also physically, e.g. it has been shown (Bechert & Pfizenmaier 1975) that the transition from laminar to turbulent flow can be triggered by sound pulses with an energy input much smaller than that associated with changes in the flow structure. The aim in the present paper is to concentrate on sound propagation in a shear flow, rather than the triggering of instabilities by sound, i.e. the non-resonant part of the spectrum. Nevertheless, it is worth noting that the stability problem for an inviscid incompressible exponential shear layer can be solved in terms of Gaussian hypergeometric functions (Hughes & Reid 1965); the present case of a compressible inviscid shear layer requires the introduction of a new class of special functions, which may be called the extended hypergeometric type since they satisfy a second-order differential equation, with two regular and one irregular singularities. The designation extended hypergeometric function is intended to distinguish it from a different case, namely the generalized hypergeometric functions (Bailey 1935; Erdelyi 1953), which have three regular singularities and satisfy differential equations of order higher than the second. The consideration of the singularities of the wave equation is important, since it specifies the wave field in the neighbourhood of the critical layer, and also asymptotically at infinity, i.e. in the free stream or far below the wall (which may affect the flow region).

The acoustic wave equation in a linear shear flow has two singularities: a regular one at the critical layer and an irregular one at infinity, where the velocity diverges. Thus by expanding around the critical layer, a solution with infinite radius of convergence is obtained which can be expressed alternatively in terms of a parabolic cylinder (Goldstein & Rice 1973), Whittaker or confluent hypergeometric (Jones 1977) functions. In the case of the exponential shear flow, the acoustic wave equation has three singularities, namely (i) at the critical layer; (ii) at the free stream; and (iii) at the opposite limit of high vorticity. The latter singularity is irregular, in contrast to the former two, which are regular. Thus the problem cannot be reduced (Ince 1926) into a confluent hypergeometric equation, nor even to a Gaussian hypergeometric equation, which has three regular singularities (Whittaker & Watson 1927). It has a higher level of complexity, between the Mathieu and Hill equations, in the sense that (i) they all have two regular singularities; (ii) the irregular singularity is of degree (Forsyth 1902) one in Mathieu's equation, degree two in the present case and of an arbitrary degree for Hill's equation. The present case can be called an extended hypergeometric equation, because it retains some properties from the particular Gaussian hypergeometric case, e.g. the extended hypergeometric equation transforms into itself under some of the six coordinate transformations of the Kleinian group (Erdelyi 1953), which leave invariant the three singular points $0, 1, \infty$. Thus solutions can be obtained by the Frobenius–Fuchs method (Forsyth 1927) near (i) the free stream, showing the existence of (a) outward and inward propagating waves, or (b) of surface guided modes; and (ii) the critical layer where there is a logarithmic singularity, and a jump in wave amplitude, due to partial absorption of the wave. The Frobenius–Fuchs method fails completely near the irregular singularity, where the method of normal integrals yields an asymptotic solution, and the solution using infinite determinants (Forsyth 1902) can be obtained directly, or by reduction to Hill's equation. It is shown, however, that there are cases for which the latter solution is not needed, because the whole flow region can be covered by analytic continuation, involving one pair of solutions of type (i) and/or one pair of solutions of type (ii). These two sets of solutions are illustrated by plots of the acoustic pressure as a function of distance from the wall for various combinations of wave frequency, horizontal wavenumber, shear-layer thickness and free-stream Mach number. The present paper concentrates on the physical properties of sound in an exponential shear flow, and relegates to a related future paper some mathematical aspects of the solution of the extended hypergeometric differential equation.

The paper is organized as follows: in § 2, the existence of a critical layer, for the acoustic wave equation in a unidirectional shear flow is demonstrated in general, and for linear and exponential velocity profiles, and its significance is discussed in terms of the ray approximation and exact solutions; in § 3, besides the regular singularity at the critical layer, we show that the wave equation has another regular singularity in the free stream, and an irregular singularity below the wall, so that analytic continuation between pairs of solutions covers the whole flow region; § 4 shows that using these three pairs of solutions it is always possible to apply boundary conditions, and plot the acoustic pressure as a function of distance from the wall, for all combinations of parameters of the problem, namely, wave frequency and horizontal wavenumber, shear-layer thickness, free-stream velocity and sound speed; in § 5, the calculation and plots of the solutions around the free stream, which represents either outward or inward propagating waves or surface (guided) modes, are considered first; then in

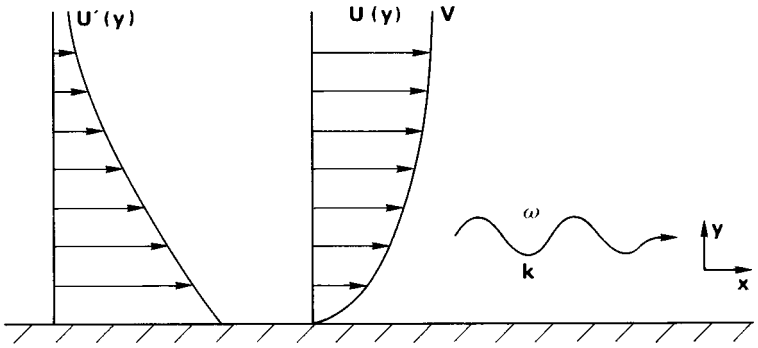

Figure 1. Sound wave of frequency ω and horizontal wavenumber k in an exponential shear flow.

§ 6, since the former solutions have their radius of convergence limited by the critical layer, next solutions are obtained which are valid around the critical level, where waves can be absorbed; in § 7 in the plots, the acoustic pressure is put into a dimensionless form by dividing by its value in the free stream, and rigid and impedance wall conditions are used; finally, in § 8, we discuss an exceptional case, when a solution in terms of Bessel functions applies over the whole flow region, when the two regular singularities coincide, i.e. when the critical layer lies in the free stream. The solution of the extended hypergeometric equation, and the mathematical properties of the extended hypergeometric functions, which appear in the present acoustic problem, are discussed in more detail in a future paper.

Part I. General properties

Following the introduction, the general properties of sound in a unidirectional shear flow are first discussed, with particular reference to the exponential profile, namely: (§ 2) the existence of a critical layer and its physical implications; (§ 3) the sets of solutions of the wave equation and analytic continuation between them; (§ 4) some possible choices of conditions to determine the constants of integration, e.g. radiation or boundedness conditions in the free stream; absence or presence of logarithmic singularity at the critical layer; and moving, impedance or rigid walls.

2. Existence of a critical layer

The two-dimensional linearized inviscid momentum equations are

$$\frac{\mathrm{d}u}{\mathrm{d}t} + U'v + \rho^{-1}\frac{\partial p}{\partial x} = 0, \tag{2.1a}$$

$$\frac{\mathrm{d}v}{\mathrm{d}t} + \rho^{-1}\frac{\partial p}{\partial y} = 0, \tag{2.1b}$$

where u, v are the components of the acoustic velocity, p is the acoustic pressure, ρ is the mean flow mass density and $\mathrm{d}/\mathrm{d}t$ is the material derivative (2.2 *a*):

$$\frac{\mathrm{d}}{\mathrm{d}t} \equiv \frac{\partial}{\partial t} + U\frac{\partial}{\partial x}, \tag{2.2a}$$

$$U \equiv U(y)\boldsymbol{e}_x \tag{2.2b}$$

for (figure 1) unidirectional shear flow (2.2 *b*), with velocity $U(y)$, in the x-direction. In adiabatic conditions, the equation of continuity reads (2.3 *a*)

$$c^{-2}\frac{\mathrm{d}p}{\mathrm{d}t}+\rho' v+\rho\left(\frac{\partial u}{\partial x}+\frac{\partial v}{\partial y}\right)=0, \tag{2.3a}$$

$$c^2\equiv\left(\frac{\partial p_o}{\partial \rho}\right)_{\mathrm{s}}, \tag{2.3b}$$

where c is the sound speed, calculated from the mean flow pressure p_0. For a low Mach number mean flow, the sound speed c and mass density ρ do not depend on distance from the wall, unlike the mean flow velocity $U(y)$ without restriction of the Mach number, if the mean flow is homentropic, $s=$ const., since the pressure is also constant, the equation of state implies that c and ρ are constant too. In (2.1 *a*), (2.3 *a*), primes denote derivative with regard to y of mean state variables, e.g. $U'\equiv \mathrm{d}U/\mathrm{d}y$, in the commutation rules:

$$\frac{\mathrm{d}}{\mathrm{d}t}\frac{\partial}{\partial x}=\frac{\partial}{\partial x}\frac{\mathrm{d}}{\mathrm{d}t}, \tag{2.4a}$$

$$\frac{\mathrm{d}}{\mathrm{d}t}\frac{\partial}{\partial y}=\frac{\partial}{\partial y}\frac{\mathrm{d}}{\mathrm{d}t}-U'\frac{\partial}{\partial x}; \tag{2.4b}$$

bearing these in mind, (2.1), (2.3 *a*) can be eliminated for the acoustic pressure, leading to the wave equation (Pridmore-Brown 1958; Lilley 1973; Mohring *et al.* 1983) in a unidirectional shear flow:

$$\frac{\mathrm{d}\left(c^{-2}\dfrac{\mathrm{d}^2p}{\mathrm{d}t^2}-\nabla^2p\right)}{\mathrm{d}t}+2U'\frac{\partial^2p}{\partial x\partial y}=0. \tag{2.4c}$$

In the absence of shear flow $U'=0$, this simplifies to the convected wave equation, in brackets, which is of second order; the interaction of sound with vorticity raises the acoustic wave equation to the third order, by coupling acoustic waves and vortical modes. Since the mean state does not depend on time and longitudinal coordinates, it is convenient to use a double Fourier integral representation:

$$P(x,y,t)=\iint_{-\infty}^{+\infty}P(y;k;\omega)\mathrm{e}^{\mathrm{i}(kx-\omega t)}\,\mathrm{d}k\mathrm{d}\omega, \tag{2.5}$$

where $P(y;k,\omega)$ denotes the acoustic pressure spectrum, for a wave of frequency ω and longitudinal wavenumber k, at a transverse position y. Substituting (2.5) into (2.4 *c*) yields the acoustic wave equation for the acoustic pressure spectrum:

$$(\omega-kU)P''+2kU'P'+(\omega-kU)[(\omega-kU)^2/c^2-k^2]P=0, \tag{2.6}$$

valid for a low Mach number unidirectional shear flow (Mohring *et al.* 1983) or for an homentropic mean flow without restriction on the Mach number.

The coefficient of P'' in (2.6) is the Doppler shifted frequency (2.7 *a*)

$$\omega_*(y)\equiv\omega-kU(y), \tag{2.7a}$$

$$\omega_*(y_{\mathrm{c}})=0, \tag{2.7b}$$

and where it vanishes (2.7 *b*), a critical layer $y=y_{\mathrm{c}}$ exists. In the case of a linear velocity profile (2.8 *a*) with vorticity q,

$$U(y)=-qy, \tag{2.8a}$$

$$y_{\mathrm{c}}=\omega/kq, \tag{2.8b}$$

a critical layer always exists (2.8 *b*). If the linear velocity profile is matched to a uniform stream (2.9 *a*),

$$U(y) = \begin{cases} Vy/h, & \text{if } 0 \leqslant h, \\ V, & \text{if } y \geqslant h, \end{cases} \tag{2.9a}$$

$$q(y) = \begin{cases} -V/h, & \text{if } 0 \leqslant h, \\ 0, & \text{if } y \geqslant h, \end{cases} \tag{2.9b}$$

the vorticity (2.9 *b*) vanishes in the uniform stream, and a critical layer exists if $y_c \leqslant h$, i.e. if the Doppler shifted frequency is non-positive in the free stream $\omega - kV \leqslant 0$. The same condition applies (figure 1) to a unidirectional exponential shear flow:

$$U(y) = V(1 - \mathrm{e}^{-y/L}), \tag{2.10a}$$

$$q(y) = -(V/L)\mathrm{e}^{-y/L}, \tag{2.10b}$$

for which the free-stream velocity V and shear-layer thickness L can be chosen independently, and the vorticity decays smoothly, from $-V/L$ at the wall, to zero in the free stream. The Doppler shifted frequency,

$$\omega = \omega_*(0) \geqslant \omega_*(y) = \omega - kV + kV\mathrm{e}^{-y/L} \geqslant \omega_*(\infty) = \omega - kV, \tag{2.11}$$

is maximum at the wall, where it equals the wave frequency ω, and minimum at the free stream, where the Doppler shift is largest; the critical layer is located at

$$y_c = -L\log(1 - \Omega), \tag{2.12a}$$

$$\Omega \equiv \omega/kV, \tag{2.12b}$$

showing that there are two cases: (i) if the Doppler shifted frequency is positive in the free stream $\omega > kV$, then it is positive everywhere, and there is no critical layer, namely the y_c complex in (2.12 *a*) for $\Omega > 1$; (ii) if the Doppler shifted frequency is negative in the free stream $\omega < kV$, then, since it is positive at the wall, it must vanish at an intermediate position, namely y_c is real for $\Omega < 1$. The intermediate case $\Omega = 1$ would correspond to a critical layer in the free stream (see § 8). In the preceding discussion it has been assumed that the horizontal wavenumber is positive $k = |k| > 0$, corresponding to propagation in the positive x-direction, i.e. parallel to the mean flow, so that the Doppler shifted frequency cannot exceed the wave frequency, $\omega_*(y) = \omega - |k|U(y) < \omega$; in the opposite case $k = -|k| < 0$, of propagation in the negative x-direction, the Doppler shifted frequency exceeds the wave frequency $\omega_*(y) = \omega + |k|U(y) \geqslant \omega$; thus it never vanishes, and no critical layer can exist.

To describe the acoustics of the exponential boundary layer, taking into account the possible existence of a critical layer, requires an exact solution of the acoustic wave equation (2.6), for (2.10 *a*) the exponential shear flow:

$$\left\{\frac{1 - \mathrm{e}^{-y/L}}{1 - \Omega}\right\}P'' - \frac{2}{L}\left\{\frac{\mathrm{e}^{-y/L}}{1 - \Omega}\right\}P' + \left[\frac{1 - \mathrm{e}^{-y/L}}{1 - \Omega}\right]\left\{\left[(1 - \Omega + \mathrm{e}^{-y/L})\frac{V}{c}\right]^2 - 1\right\}k^2P = 0. \tag{2.13}$$

The form of the coefficients suggests the change of independent variable (2.14 *a*), which measures distance from the wall in the same scale as the vorticity (2.10 *b*), and

has a coefficient such that the critical layer (2.12 *a*) lies at position unity $\zeta(y_c) = 1$, namely

$$\zeta = \frac{e^{-y/L}}{1-\Omega} = e^{-(y-y_c)/L}, \tag{2.14 a}$$

$$p(y;k,\omega) = f(\zeta); \tag{2.14 b}$$

thus (2.13) leads to a differential equation with polinomial coefficients:

$$(1-\zeta)\zeta^2 f'' + \zeta(1+\zeta)f' + (1-\zeta)\{\Lambda^2(1-\zeta)^2 - K^2\}f = 0, \tag{2.15}$$

which involves two dimensionless parameters

$$\Lambda \equiv (\omega - kV)L/c, \tag{2.16 a}$$

$$K \equiv kl, \tag{2.16 b}$$

namely the Doppler shifted frequency (2.16 *a*) and horizontal wavenumber (2.16 *b*). The differential equation (2.15) has cubic polynomial coefficients, whose degree can be reduced by one unit, via the change of dependent variable (2.17 *a*):

$$f(\zeta) = \zeta^{\vartheta} g(\zeta), \tag{2.17 a}$$

$$\zeta^{\vartheta} \sim e^{-\vartheta y/L}, \tag{2.17 b}$$

which is equivalent to the introduction of an exponential factor (2.17 *b*), where the constant ϑ may be chosen at will. Substituting (2.17 *a*) in (2.15) yields

$$(1-\zeta)\zeta^2 g'' + \zeta\{(1+2\vartheta) + \zeta(1-2\vartheta)\}g' + \{\Lambda^2(1-\zeta)^3 + (\vartheta^2 - \vartheta - K^2)(1-\zeta) + \vartheta(1+\zeta)\}g = 0; \tag{2.18}$$

if ϑ is chosen so as to cancel the terms in the last curly brackets, which are independent of ζ,

$$\Lambda^2 + \vartheta^2 - K^2 = 0, \tag{2.19 a}$$

$$\vartheta = \sqrt{K^2 - \Lambda^2}, \tag{2.19 b}$$

then the differential equation (2.18) can be divided by ζ, and its coefficients become quadratic:

$$(1-\zeta)\zeta g'' + \{(1+2\vartheta) + \zeta(1-2\vartheta)\}g' + \{2\vartheta - \Lambda^2(1-\zeta)(2-\zeta)\}g = 0, \tag{2.20}$$

with the leading coefficient as in the Gaussian hypergeometric equation.

Before proceeding to solve exactly the differential equation (2.20), it is worth while considering the leading term of the solution in the neighbourhood of the free stream $y = \infty$ or $\zeta = 0$ by (2.14 *a*). Writing the differential equation (2.20) in the form

$$\zeta^2 g'' + \zeta r_0(\zeta) g' + s_0(\zeta) g = 0, \tag{2.21}$$

where

$$r_0(\zeta) \equiv 2\vartheta + (1+\zeta)/(1-\zeta), \tag{2.22 a}$$

$$s_0(\zeta) \equiv \zeta[2\vartheta/(1-\zeta) - \Lambda^2(2-\zeta)], \tag{2.22 b}$$

are analytic at $\zeta = 0$, it follows that the latter is a regular singularity, and a power series solution exists in its vicinity:

$$g(\zeta) = \zeta^{\sigma} \sum_{n=0}^{\infty} a_n(\sigma)\zeta^n. \tag{2.23}$$

The leading term $\zeta^\sigma = \mathrm{e}^{-\sigma y/L}$ is specified by σ, which is a root of the indicial equation

$$0 = \sigma(\sigma - 1) + \sigma r_0(0) + s_0(0) = \sigma(\sigma + 2\vartheta). \tag{2.24}$$

Thus $\sigma = 0, -2\vartheta$, and the two particular integrals scale (2.14 *b*), (2.17 *a*), (2.23) as

$$P_\pm(y \to \infty; k, \omega) \sim \zeta^{\vartheta+\sigma} = \zeta^{\pm\vartheta} \sim \mathrm{e}^{\mp\vartheta y/L}, \tag{2.25}$$

in the neighbourhood of the free stream, where the mean flow velocity is $V = U(\infty)$ in the free stream, and thus the transverse wavenumber $\bar{k}$, in the y-direction, is given by

$$\bar{k} = \sqrt{(\omega - kV)^2/c^2 - k^2}. \tag{2.26}$$

Thus the acoustic pressure spectrum (2.5), in the ray limit of wavelength that is small compared to the length-scale of change of the mean flow velocity, is given by

$$P(y \to \infty; k, \omega) \sim \mathrm{e}^{\pm \mathrm{i}\bar{k}y}; \tag{2.27}$$

the ray limit applies in the free stream, as can be confirmed by comparing (2.27) and (2.25), namely

$$\bar{k} = -\mathrm{i}\vartheta/L = -\mathrm{i}\sqrt{k^2 - \Lambda^2/L^2}, \tag{2.28}$$

coincides with (2.26) when (2.19 *b*), (2.16) are used. Thus the leading term of the exact acoustic field (2.14 *b*), (2.17 *a*), (2.23) in the neighbourhood of the free stream, is the ray solution (2.26), (2.27). If the transverse wavenumber in the ray limit is imaginary $\bar{k} = \pm\mathrm{i}|\bar{k}|$, then $\vartheta = \mathrm{i}\bar{k}L = \mp|\bar{k}|L$ is real, all coefficients of the wave equation (2.20) are real and no propagating waves exist; the wave field scales as $\exp(\mp|k|y)$ as $y \to \infty$ and a bounded acoustic field (choice of 'minus' sign) implies surface modes in the boundary layer; this is the case when (2.26) is imaginary, i.e. $|\omega - kV| < kc$ or $|\Omega - 1| < 1/M$ using (2.12 *b*) and the Mach number in the free stream

$$M^2 \ll 1, \qquad M \equiv V/c, \tag{2.29}$$

which is restricted to low values, $M \leqslant \frac{1}{3}$, by the assumption of incompressible mean flow. The condition $\Omega < 1 + 1/M$ with $M = \frac{1}{3}$, shows that only surface waves are possible for $\Omega < 4 \equiv \Omega_*$, i.e. including all cases where a critical layer exists $\Omega \leqslant 1$. Propagating waves are possible in the opposite case of real $\bar{k}$, imaginary ϑ and $\Omega > 1 + 1/M > \Omega_*$, but this can occur only in the absence of a critical layer $\Omega > 1$. These conclusions are summarized in the table:

waves	propagating	surface
condition	$\lvert\Omega - 1\rvert > 1/M$	$\lvert\Omega - 1\rvert < 1/M$
frequency	$\Omega > 1 + 1/M \equiv \Omega_*$	$\Omega < 1 + 1/M \equiv \Omega_*$
spectrum	$\omega > k(V + c) \equiv \omega_*$	$\omega < k(V + c) \equiv \omega_*$
critical layer	never	possible ($\Omega \leqslant 1$)

(2.30)

and also in figure 2, where the spectrum is split into propagating waves at 'high' frequencies and surface waves at 'low' frequencies, separated by the 'cut-off frequency':

$$\Omega_* \equiv 1 + 1/M, \tag{2.31 a}$$

$$\omega_* \equiv k(V + c). \tag{2.31 b}$$

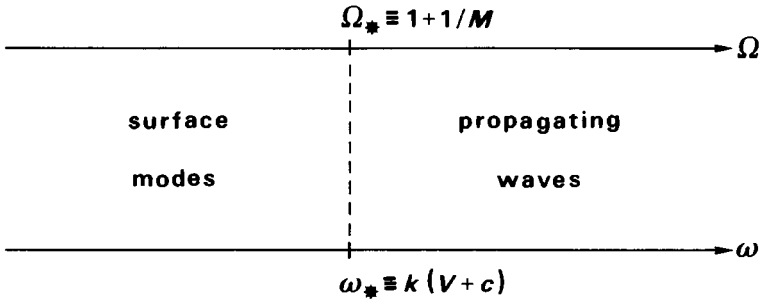

Figure 2. The spectrum is split into propagating waves and surface modes, respectively, above and below a cut-off frequency calculated for free stream.

This 'cut-off frequency' is not comparable to those applying to the acoustics of ducts (Ballantine 1927; Tsien 1952; Eisenberg & Kao 1971; Nayfeh *et al*. 1975; Campos 1984, 1985*a*, 1986*a*, *b*, 1987*b*; Campos & Lau 1996*a*, *b*) or to waves in an atmosphere (Moore & Spiegel 1964; Lighthill 1978; Campos 1983*d*, 1985*b*, 1987*a*, 1991; Campos & Saldanha 1991); the latter cut-off frequencies are determined by lengthscales of variations of properties of the media.

3. Solutions of the wave equation

The radius of convergence of the solution (2.23) around the free stream $|\zeta| < 1$ is limited by the critical layer $\zeta(y_c) = 1$, when the latter exists. In order to study the behaviour of the wave field near the critical layer, the independent variable is changed to (3.1 *a*)

$$\xi = 1 - \zeta, \tag{3.1a}$$

$$g(\zeta) = h(\xi), \tag{3.1b}$$

so that the differential equation (2.20) becomes

$$(1-\xi)\xi h'' - \{2 + \xi(1-2\vartheta)\}h' + \{2\vartheta - \Lambda^2\xi(1+\xi)\}h = 0. \tag{3.2}$$

Writing (3.2) in the form

$$\xi^2 h'' + \xi r_1(\xi) h' + s_1(\xi) h = 0, \tag{3.3}$$

where

$$r_1(\xi) \equiv -\frac{2 + \xi(1-2\vartheta)}{1-\xi}, \tag{3.4a}$$

$$s_1(\xi) \equiv \frac{2\vartheta - \Lambda^2\xi(1+\xi)}{1/\xi - 1}, \tag{3.4b}$$

are analytic at $\xi = 0$, it follows that the critical layer ($\zeta = 1$ or $y = y_c$) is a regular singularity, and a solution exists in the form

$$h(\xi) = \xi^\sigma \sum_{n=0}^{\infty} b_n(\sigma)\xi^n, \tag{3.5}$$

where the indices are the roots of

$$0 = \sigma(\sigma-1) + \sigma r_1(0) + s_1(0) = \sigma(\sigma-3). \tag{3.6}$$

Since the indices differ by the integer 3, one particular integral is a series starting at the third power:

$$P_1(y;k,\omega) \sim \xi^3 = \{1-\exp[(y_c-y)/L]\}^3 \sim [(y_c-y)/L]^3, \tag{3.7}$$

and the other

$$P_2(y;k,\omega) \sim \xi^3 \log \xi + O(1), \tag{3.8}$$

has a logarithmic term. It is clear that (3.7) vanishes as $\xi \to 0$, at the critical layer, and (3.8) is finite. In order to interpret the logarithmic term in (3.8) it is usual (Booker & Bretherton 1976; McKenzie 1979), in the absence of dissipation (fluid viscosity and thermal conduction in this case), to give the frequency a small positive imaginary part $\bar{\omega} = \omega + \mathrm{i}\varepsilon$, to simulate the onset of an instability $\exp(-\mathrm{i}\bar{\omega}t) = \exp(-\mathrm{i}\omega t)\exp(\varepsilon t)$ for $\varepsilon > 0$. In the case of a stable system, which has no poles in the upper complex ω-plane, the path of integration along the real ω-axis in (2.5) can be shifted to $+\mathrm{i}\omega$, giving a zero wave field for $t < 0$, as required by causality. An incompressible inviscid shear layer is stable, but this may not be the case in the compressible case, i.e. sound may trigger flow instabilities, which in turn amplify the sound field (Jones 1977); this would be represented by the poles of the integrand in the upper complex ω-plane. Since the present paper is not concerned with the instabilities, but only with the non-resonant part of the spectrum, one may proceed to substitute $\bar{\omega} = \omega + \mathrm{i}\varepsilon$ in (2.12 *a*), so that the location of the critical layer is shifted to

$$\bar{y}_c \equiv -L\log\left(1-\frac{\bar{\omega}}{kV}\right) = -L\log\left(1-\frac{\omega}{kV}-\frac{\mathrm{i}\varepsilon}{kV}\right) \sim y_c + \frac{\mathrm{i}\varepsilon L}{kV-\omega}, \tag{3.9}$$

since the critical layer exists for $kV > \omega$, the imaginary part of $\bar{y}_c$ is positive, then $\mathrm{Im}\{(y-\bar{y}_c)/L\} < 0$, and in the logarithmic term in (3.8), the argument is $-\mathrm{i}\pi$ as $y \to y_c - 0$, namely

$$\log\xi \sim \log\{(y-y_c)/L\} = \begin{cases} \log\{|y-y_c|/L\}, & \text{if } y > y_c, \\ \log\{|y-y_c|/L\} - \mathrm{i}\pi, & \text{if } y < y_c. \end{cases} \tag{3.10}$$

Thus there is a phase jump of π rad (180°) when crossing the critical layer from the wall to the free stream, and a jump of $-\pi$ in the opposite direction.

The differential equation (2.20) has a third singularity at infinity $\zeta = \infty$, which is mapped to the origin $\eta = 0$ by the change of variable

$$\eta = 1/\zeta, \tag{3.11 a}$$

$$j(\eta) = g(\zeta), \tag{3.11 b}$$

which transforms (2.20) to

$$\eta^2(1-\eta)j'' + \eta\{3-2\vartheta+\eta(2\vartheta-1)\}j' + \left\{2\vartheta - \Lambda^2\left(2-\frac{3}{\eta}+\frac{1}{\eta^2}\right)\right\}j = 0. \tag{3.12}$$

Writing this equation in the form

$$\eta^2 j'' + r_\infty(\eta)\eta j' + s_\infty(\eta) j = 0, \tag{3.13}$$

where

$$r_\infty(\eta) = \frac{3-2\vartheta+\eta(2\vartheta-1)}{1-\eta} \tag{3.14 a}$$

$$s_\infty(\eta) = \frac{2\vartheta - \Lambda^2\left(2-\frac{3}{\eta}+\frac{1}{\eta^2}\right)}{1-\eta}, \tag{3.14 b}$$

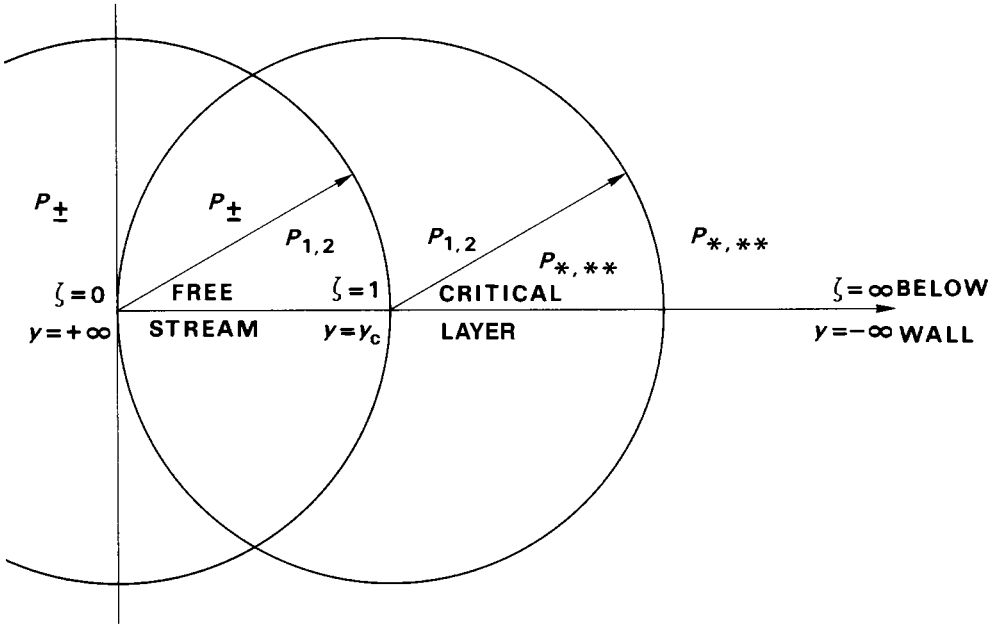

Figure 3. The ζ-plane of flow region $y > 0$ is covered by three pairs of solutions, valid near the free stream and critical layer, which are regular singularities, and near the irregular singularity, in the limit of strong vorticity, below the wall.

it follows that, since $\Omega \neq 1$ in (2.12 *a*) and $\Lambda \neq 0$ in (2.16 *a*), the function (3.14 *b*) is not analytic at $\eta = 0$, and the latter is an irregular singularity. Note that if $\Lambda = 0$, then (2.20) would have been a Gaussian hypergeometric equation, which has regular singularities at $\zeta = 0, 1, \infty$. The present equation is of the extended hypergeometric type, in the sense that it differs from the hypergeometric type, in that the coefficient of g has terms of $O(\zeta)$ and $O(\zeta^2)$. Thus the present equation is of a higher degree than Mathieu's equation, which has a term of $O(\zeta)$ in Lindeman's form (Whittaker & Watson 1927), but of a lower degree than Hill's equation, which has terms of all orders $O(\zeta^n)$, with n integer (Ince 1926). This question is pursued further in a future paper, where the mathematical properties of the extended hypergeometric equation are discussed, including behaviour at infinity. It can be shown that (i) the Frobenius–Fuchs method fails to give any particular integral, i.e. there is no power series solution; (ii) a solution in the form of a normal integral exists, but it provides an asymptotic expansion, i.e. it does not converge as a descending series; (iii) Laurent series solutions exist, but they involve infinite systems of equations, and infinite determinants, as for Hill's equation.

Concerning the present acoustic problem, the aim is to obtain the simplest set of solutions, which covers the whole flow region, for every possible combination of parameters. The differential equation (2.20) has singularities at the points $\zeta = 0, 1, \infty$, which are the fixed or invariant points (Erdelyi 1953) of the Kleinian group of transformations:

$$\zeta \to 1 - \zeta, \frac{1}{\zeta}, 1 - \frac{1}{\zeta}, \frac{1}{1-\zeta}, \frac{\zeta}{1-\zeta}. \tag{3.15}$$

Thus a pair of solutions in each of these six variables could be considered, i.e. two pairs in the neighbourhood of each singularity; it follows by analytic continuation (figure 3) that any solution is a linear combination of any pair of solutions. If the aim is to cover the whole complex ζ-plane, a pair of solutions is needed in the neighbourhood of each singularity, namely using ζ or $\zeta/(1-\zeta)$ near $\zeta = 0$, and $1-\zeta$ or $1-1/\zeta$ near $\zeta = 1$, and $1/\zeta$ or $1/(1-\zeta)$ near $\zeta = \infty$. In the case of the Gaussian hypergeometric equation, it transforms into itself via any transformation of the Kleinian group (3.15), because the three fixed points $\zeta = 0, 1, \infty$ are all regular singularities. In the present case, of the extended hypergeometric equation, the fixed point $\zeta = \infty$ is an irregular singularity, and the equation transforms into itself (2.20), (3.2) only for one change of variable, namely (3.1 *a*), which interchanges the two regular singularities $\zeta = 0, 1$. The remaining changes of variable in (3.15), i.e. all but the first, lead to a differential equation which is no longer of the extended hypergeometric type, e.g. (3.12) for (3.11 *a*), which is the second change of variable in (3.15). As a further example, consider a second pair of solutions in the neighbourhood of the critical layer, i.e. distinct from (3.1 *a*), (3.2), (3.5), (3.6); among the changes of variable in (3.15), the choice distinct from (3.1 *a*) is

$$\chi = 1 - \frac{1}{\zeta} = 1 - \eta, \tag{3.16 a}$$

$$\ell(\chi) = j(\eta), \tag{3.16 b}$$

which transforms equation (3.12) to

$$\chi(1-\chi)^4\ell'' - (1-\chi)^3\{2 + (1-2\vartheta)\chi\}\ell' + \{2(\vartheta - \Lambda^2)(1-\chi)^2 + 3\Lambda^2\}\ell = 0, \tag{3.17}$$

which is no longer of the extended hypergeometric type. The critical layer $\chi = 0$ is still a regular singularity, and the indicial equation $\sigma(\sigma - 3) = 0$ the same; the implication is that in both cases a logarithmic singularity exists at the critical layer (3.8). It may be expected that both solutions, of (3.2) and (3.17), have similar behaviour in the neighbourhood of the regular singularity, $\zeta = 1$, $\xi = 0$ and $\chi = 0$, but that their radius of convergence is different, namely: (i) for (3.2), the singularity nearest to $\zeta = 1$, $\xi = 0$ is $\zeta = 0$, $\xi = 1$, which is regular, and thus the radius of convergence is unity $|\xi| < 1$, as will be confirmed subsequently (see § 6); (ii) for (3.17), the singularity nearest to $\chi = 0$, $\zeta = 1$ is $\chi = 1$, $\zeta = \infty$, which is irregular, and thus the solution about $\chi = 0$ cannot represent a solution near $\chi = 1$, and the radius of convergence must be less than unity. Thus the former solution has a larger radius of convergence. In conclusion, a good choice of the three pairs of solutions to cover the whole ρ-plane is those of (2.20), (3.2) and (3.12).

Denoting by P_* and P_{**} two linearly independent solutions of the last differential equation (3.12), the acoustic pressure is given by a linear combination:

$$P(y; k, \omega) = C_* P_*(y; k, \omega) + C_{**} P_{**}(y; k, \omega), \tag{3.18 a}$$

where C_*, C_{**} are arbitrary constants; the solution is valid for

$$-1 < \frac{1}{\zeta} = (1-\Omega)\mathrm{e}^{y/L} = \exp\left\{\frac{y - y_\mathrm{c}}{L}\right\} < 1. \tag{3.18 b}$$

The other pair of solutions (3.7), (3.8) about the critical layer, specifies the acoustic pressure

$$P(y; k, \omega) = C_1 P_1(y; k, \omega) + C_2 P_2(y; k, \omega) \tag{3.19 a}$$

in the region

$$-1 < 1 - \zeta = 1 - \frac{\mathrm{e}^{-y/L}}{1-\Omega} = 1 - \exp\left\{-\frac{y-y_\mathrm{c}}{L}\right\} < 1; \tag{3.19 b}$$

the solution (2.25) about the free stream, specifies the acoustic pressure

$$P(y;k,\omega) = C_+ P_+(y;k,\omega) + C_- P_-(y;k,\omega) \tag{3.20 a}$$

in the region

$$-1 < \zeta = \frac{\mathrm{e}^{-y/L}}{1-\Omega} = \exp\left\{-\frac{y-y_\mathrm{c}}{L}\right\} < 1. \tag{3.20 b}$$

The three solutions (3.18 *a*), (3.19 *a*), (3.20 *a*) are valid in the overlapping regions (3.18 *b*), (3.19 *b*), (3.20 *b*), and thus are (figure 3) analytic continuations of each other. It follows that any of these six functions $P_+, P_-, P_*, P_{**}, P_1, P_2$ is a linear combination of any pair (P_+, P_-), (P_*, P_{**}), (P_1, P_2), with definite coefficients

	P_+	P_-	P_1	P_2	P_*	P_{**}
P_+	1	0	C_{+1}	C_{+2}	C_{+*}	C_{+**}
P_-	0	1	C_{-1}	C_{-2}	C_{-*}	C_{-**}
P_1	C_{1+}	C_{1-}	1	0	C_{1*}	C_{1**}
P_2	C_{2+}	C_{2-}	0	1	C_{2*}	C_{2**}
P_*	C_{*+}	C_{*-}	C_{*1}	C_{*2}	1	0
P_{**}	C_{**+}	C_{**-}	C_{**1}	C_{**2}	0	1

(3.21)

which can be determined by comparing the two sides at two points. For example, the coefficients in the relation

$$P_1(y;k,\omega) = C_{1+} P_+(y;k,\omega) + C_{1-} P_-(y;k,\omega) \tag{3.22}$$

can be determined by solving at two points y_1, y_2 in the intersection of the regions of validity:

$$\begin{bmatrix} C_{1+} \\ C_{1-} \end{bmatrix} \{P_+(y_1)P_-(y_2) - P_-(y_1)P_+(y_2)\} = \begin{bmatrix} P_-(y_2) & -P_-(y_1) \\ -P_+(y_2) & P_+(y_1) \end{bmatrix} \begin{bmatrix} P_1(y_1) \\ P_1(y_2) \end{bmatrix}. \tag{3.23}$$

Using the relations (3.21), of type (3.22), with definite coefficients like (3.23), any pair of constants of integration (C_1, C_2) in (3.19 *a*), $C_\pm$ in (3.20 *a*) and (C_*, C_{**}) in (3.18 *a*) can be expressed in terms of any other pair; for example, if $C_\pm$ are given, then C_1, C_2, C_*, C_{**} can be determined using the coefficients in (3.21). It follows that there are only two independent arbitrary constants of integration, as there should be for the solution of a second-order differential equation.

4. Boundary and radiation conditions

Thus two boundary conditions are needed to determine all arbitrary constants of integration in (3.18 *a*), (3.19 *a*), (3.20 *a*), and it does not matter where these conditions are specified, because there are connecting formulae (3.21) across the whole flow region. The examples of possible boundary conditions which will be given next apply at the free stream, at the critical layer and at the wall. Concerning the vicinity

of the free stream (3.20 *a*), if (i) $|\Omega - 1| > 1/M$, there are outward P_+ and inward P_- propagating waves, and a radiation condition choosing the former (latter) sets $C_- = 0$ ($C_+ = 0$); and if (ii) $|\Omega - 1| < 1/M$, there are unstable P_+ and surface P_- waves, so that the pressure field is bounded only if $C_+ = 0$. Concerning the vicinity of the critical layer (3.19 *a*), the latter exists (2.12 *a*) if $\Omega < 1$, in which case (2.30) only surface waves can be considered, implying that $C_+ = 0 \neq C_-$; from (3.21) it follows that the two components of the wave field (3.7), (3.8) in the neighbourhood of the critical layer have coefficients C_-C_{-1} and C_-C_{-2}, respectively, and thus the logarithmic singularity at the critical layer cannot be avoided. In this case the critical layer can act as a partially absorbing layer, extracting some energy from the wave because there is an amplitude jump πC_-C_{-2} due to the logarithmic singularity. For propagating waves (2.30), no critical layer exists, and thus the logarithmic term (3.8) is not singular. At the wall $y = 0$, it follows from the momentum equation (2.1 *b*), (2.2 *a*) that

$$P'(0;k,\omega) = \mathrm{i}\rho[\omega - kU(0)]V(0;k,\omega), \tag{4.1 a}$$

where for an exponential boundary layer, the flow velocity (2.10 *a*) vanishes at the wall, but not the vorticity

$$P'(0;k,\omega) = \mathrm{i}\rho\omega V(0;k,\omega). \tag{4.1 b}$$

If the wall is moving with normal velocity $v(x,t)$, then its spectrum

$$V(0;k,\omega) = \frac{1}{4\pi^2}\iint_{-\infty}^{+\infty} v(x,t)\mathrm{e}^{-\mathrm{i}(kx-\omega t)}\,\mathrm{d}x\mathrm{d}t \tag{4.1 c}$$

appears in the boundary condition (4.1 *b*). If instead the wall has an impedance Z (4.2 *a*):

$$V(0;k,\omega) = Z^{-1}P(0;k,\omega), \tag{4.2 a}$$

$$ZP'(0;k,\omega) = \mathrm{i}\rho\omega P(0;k,\omega), \tag{4.2 b}$$

the boundary condition is (4.2 *b*). A particular case is the rigid wall:

$$Z = \infty, \quad V(0;k,\omega) = 0 \Leftrightarrow P'(0;k,\omega) = 0, \tag{4.3}$$

for which the normal velocity is zero, and thus the normal derivative of the pressure vanishes. The boundary condition at the wall specifies a relation between C_* and C_{**} in (3.18 *a*); the solution is made unique, by one more independent and compatible conditions, e.g. a radiation or stability condition in the free stream or absence of the logarithmic term in the neighbourhood of the critical layer. Taking the latter as an example, the condition of absence of a logarithmic term near the critical layer $C_2 = 0$, implies by (3.21) that C_* and C_{**} are proportional to C_1, so that their ratio is a constant $C_*/C_{**} = \text{const.}$; this relation, together with the linear relation between C_* and C_{**} established by the boundary condition specified at the wall, uniquely determines C_* and C_{**}. In contrast, specifying a boundary condition near the wall, and a radiation at infinity, implies that a logarithmic term will generally exist at the critical layer.

Concerning the relation between the acoustic propagation problem and the stability of the compressible shear flow, the following is an outline of how this question can be addressed. Consider an incident sound wave from the free stream, namely

$C_- = 0$ in (3.20 *a*), with a given amplitude $C_+ \neq 0$, so that the sound field is given by

$$P(y;k,\omega) = C_+ P_+(y;k,\omega) = C_+\{C_{1+}P_1(y;k,\omega) + C_{2+}P_2(y;k,\omega)\}, \tag{4.4 a}$$

where the second expression applies accross the critical layer, and generally involves a logarithmic term, because $C_+C_{2+} \neq 0$. If the second expression holds up to the wall, the third pair of solutions is not needed, and the impedance boundary condition (4.2 *b*) is independent of amplitude $C_+ \neq 0$:

$$C_{1+}P_1'(0;\omega,k) + C_{2+}P_2'(0;\omega,k) = (\mathrm{i}\rho\omega/Z)\{C_{1+}P_1(0;\omega,k) + C_{2+}P_2(0;\omega,k)\}. \tag{4.4 b}$$

The frequency ω and horizontal wavenumber k could be taken in dimensionless form (2.12 *b*), (2.16 *b*), and since the parameter (2.16 *a*) is involved in (4.4 *b*), the Mach number M and modified impedance $z \equiv Z/\rho$ also appear in the relation (4.4 *b*), leading to

$$z \equiv Z/\rho, \quad F(\omega,k,M,z) = 0, \tag{4.5}$$

which acts as a dispersion relation, and can be interpreted in two ways. First, for sinusoidal perturbations in space, it indicates their evolution in time. Taking k to be real, the roots of (4.5) are complex ω:

$$\omega \equiv \omega_\mathrm{r} + \mathrm{i}\omega_\mathrm{i}, \quad \mathrm{e}^{-\mathrm{i}\omega t} = \exp(-\mathrm{i}\omega_\mathrm{r})\exp(\omega_\mathrm{i} t), \tag{4.6 a}$$

implying that $\omega_\mathrm{r} \equiv \mathrm{Re}(\omega)$ is the frequency, and $\omega_\mathrm{i} \equiv \mathrm{Im}(\omega)$ is a growth rate in time if $\omega_\mathrm{i} > 0$, and a rate of decay if $\omega_\mathrm{i} < 0$; thus neutral stability corresponds to $\omega_\mathrm{i} = 0$. Alternatively, for sinusoidal perturbations in time, their spatial evolution can be determined. Taking ω to be real, the roots of (4.5) are complex k:

$$k \equiv k_\mathrm{r} + \mathrm{i}k_\mathrm{i}, \quad \mathrm{e}^{\mathrm{i}kx} = \exp(\mathrm{i}k_\mathrm{r}x)\exp(-k_\mathrm{i}x), \tag{4.6 b}$$

so that $k_\mathrm{r} \equiv \mathrm{Re}(k)$ is the wavenumber and $k_\mathrm{i} \equiv \mathrm{Im}(k)$ the spatial growth $k_\mathrm{i} > 0$ or decay $k_\mathrm{i} < 0$ rate; the neutral stability corresponds to $k_\mathrm{i} = 0$. In either case, the neutral stability is specified by one of the equations

$$\omega_\mathrm{i}(k,M,z) = 0, \quad k_\mathrm{i}(\omega,M,z) = 0, \tag{4.7 a}$$

whose smallest root (for k and ω, respectively) can be plotted as a curve:

$$k_*(M,z) = 0, \quad \omega_*(M,z) = 0. \tag{4.7 b}$$

Thus there will be a critical Mach number M_*, below which the shear flow is stable with regard to any acoustic perturbation. The existence of a critical Mach number is typical of shear flow stability problems. In the present case, the critical Mach number depends on the wall impedance $M_*(z)$, e.g. it could be different for a rigid wall $M_*(\infty)$, for a reactive $M_*(|R|)$ or an inductive $M_*(\mathrm{i}|R|)$ wall. Above the critical Mach number $M \geqslant M_*$, there exist pairs of frequency and wavenumber $(\omega,k)_*$ which excite shear flow instabilities, i.e. they are the resonant modes of the acoustic spectrum. The following analysis concerns the non-resonant acoustic spectrum, namely arbitrary $(\omega,k) \neq (\omega,k)_*$ excluding the resonant pairs.

It remains to be specified which solutions need to be used for the various combinations of parameters. Taking each solution in turn, and starting with the solution

(3.20 *a*) near the free stream (i) if $\Omega < 1$, it holds that $y > y_c$ above (3.20 *b*) the critical layer (2.12 *a*); and (ii) if $\Omega > 1$, it applies above the layer

$$y > y_+ \equiv -L \log(\Omega - 1), \tag{4.8}$$

and since $y_+ < 0$ for $\Omega > 2$, the latter case applies over the whole flow region. The solution (3.19 *a*) near the critical layer diverges (3.19 *b*) for $\Omega > 1$, and for $\Omega < 1$ holds in the region

$$y > y_- \equiv -L \log\{2(1 - \Omega)\} = y_c - L \log 2 = y_c - 0.693L, \tag{4.9}$$

which includes the whole flow region when $\Omega < \frac{1}{2}$, because then $y_- < 0$. The solution (3.18 *a*), near the irregular singularity, holds in opposition to (3.19 *a*), namely: (i) if $\Omega < 1$, it holds below the critical layer $y < y_c$ in (2.12 *a*); and (ii) if $\Omega > 1$, it holds below the layer (4.8):

$$y < y_+ = -L \log(\Omega - 1), \tag{4.10}$$

and since $y_+ < 0$ for $\Omega > 2$, in this case it holds nowhere in the flow region. In this case $\Omega > 2$, the solutions (3.18 *a*), (3.19 *a*) are not needed, because (3.20 *a*) covers the whole flow region. Considering the three other frequency ranges, the appropriate solutions are indicated in figure 4 and in the following table:

case	pair of solutions		
frequency range	$P_\pm$	$P_{1,2}$	P_*, P_{**}
$2 < \Omega$	$0 < y < \infty$	—	—
$1 < \Omega < 2$	$y_+ < y < \infty$	—	$0 < y < y_+$
$\frac{1}{2} < \Omega < 1$	$(y_c < y < \infty)$	$y_- < y < \infty$	$0 < y < y_c$
$\Omega < \frac{1}{2}$	$(y_c < y < \infty)$	$0 < y < \infty$	$(0 < y < y_c)$

(4.11)

Here (i) non-convergence is indicated by —; (ii) a solution which is valid, but not needed, is indicated in parentheses; and (iii) the simplest solution, or combination of solutions, which covers the whole flow region, is indicated without parentheses. The conclusion is that: (i) for $\Omega > 2$ or $\Omega < \frac{1}{2}$ the whole flow region is covered by one pair of solutions, respectively $P_\pm$ and $P_{1,2}$; (ii) two pairs can be used for $\frac{1}{2} < \Omega < 1$, namely $(P_\pm, P_{*,**})$ or $(P_{1,2}, P_{*,**})$, with the latter having a larger region of overlap; and (iii) for $1 < \Omega < 2$ the pair $(P_\pm, P_{*,**})$ can be used. Note that in the last two cases the solutions $P_{*,**}$ in the neighbourhood of the essential singularity are needed; they can be dispensed with by instead using expansions about one or more regular points, so as to cover the region $0 < y < y_c$ in case (ii), and $0 < y < y_+$ in case (iii).

Part II. Discussion of the solutions

The preceding pairs of solutions can be discussed, both analytically and in illustrations, by plots, in the following sequence: (§ 5) first the solutions in the neighbourhood of the free stream, which may consist of propagating waves (complex, with amplitude and phase) or surface modes (real); (§ 6) then the pair of solutions in the neighbourhood of the critical layer, which has a logarithmic singularity, leading to a jump of the wave field; the third set of solutions, specifying the behaviour of the wave field, in the region of vorticity, towards the wall is given in a future paper on the extended

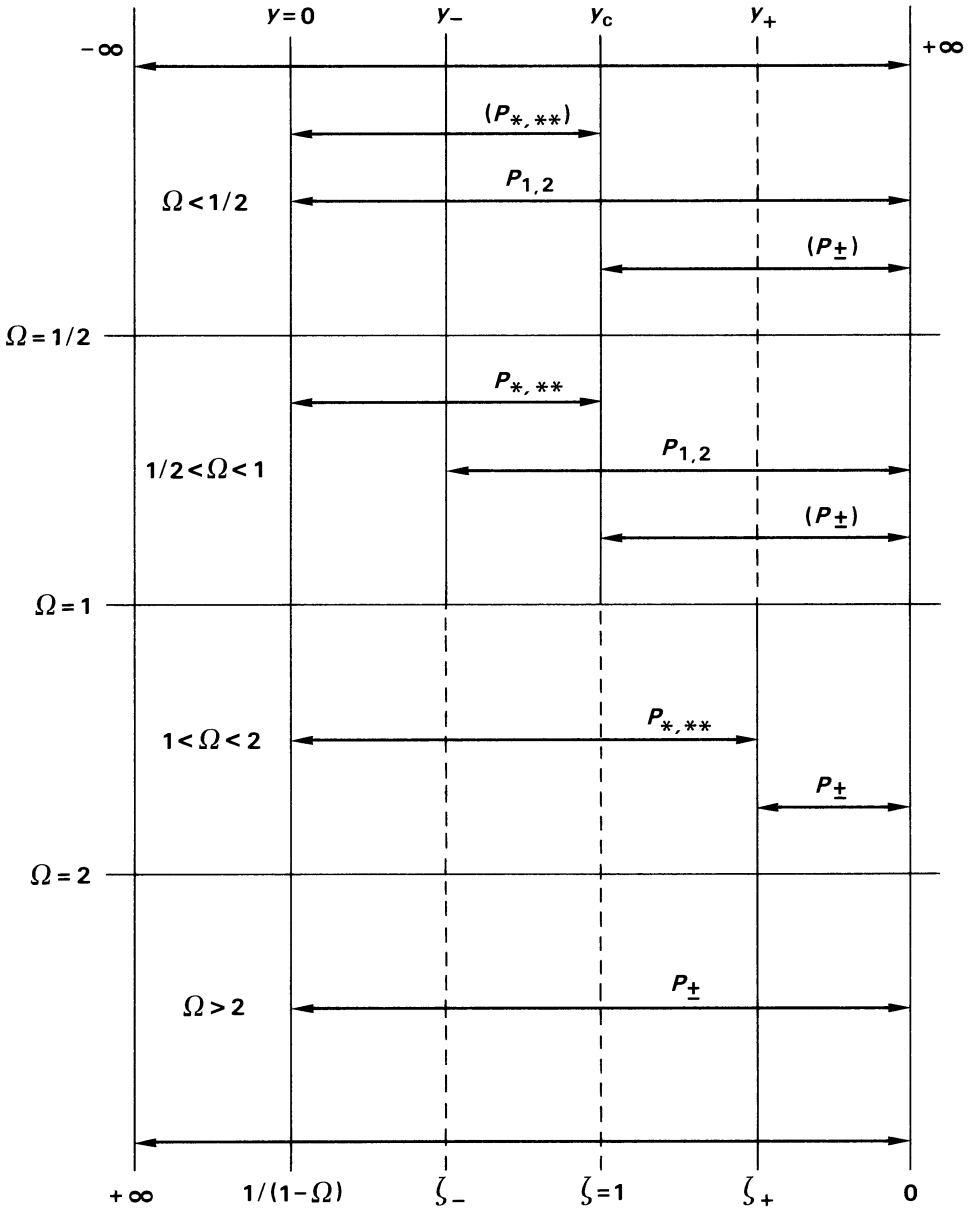

Figure 4. Flow regions where each pair of solutions converges, for each of four frequency ranges. Redundant solutions are indicated in brackets, to emphasize the others, i.e. the minimum set which covers the whole flow region.

hypergeometric equation and functions. The preceding solutions, which are plotted for rigid or impedance wall conditions (§ 7), assume that the critical layer either does not exist (i) or lies in the boundary layer (ii); the remaining possibility is for the critical level to lie in the free stream (iii), in which case the solution of the wave equations is simplest, namely is specified by Bessel functions (§ 8), because the three singularities coalesce to two.

5. Propagating and surface waves

It has been shown how the three pairs of solutions of the wave equation (§ 3) can be used to specify the wave field over the whole flow region, for various combinations of parameters and boundary conditions. The more detailed discussion of each of the pairs of solutions starts with those in the neighbourhood of the free stream, which are specified by (2.14 *b*), (2.17 *a*), (2.19 *b*) where g satisfies (2.20); the latter, on substitution of (2.23), leads to the recurrence formula

$$(n+\sigma+1)(n+\sigma+1+2\vartheta)a_{n+1} = \{(n+\sigma)(n+\sigma-2+2\vartheta)+2(\Lambda^2-\vartheta)\}a_n - 3\Lambda^2 a_{n-1} + \Lambda^2 a_{n-2}. \quad (5.1)$$

Setting $n=-1$, and noting that $a_{-1}=a_{-2}=a_{-3}=0$ because these terms do not exist in (2.23), yields $\sigma(\sigma+2\vartheta)a_0=0$; now if $a_0=0$, then all $a_n=0$, and a trivial solution is obtained. Thus $a_0\neq 0$, leading back to the indicial equation (2.24), whose roots are $\sigma=0,-2\vartheta$. In the exceptional case when $2\vartheta=m$ is an integer, one particular integral has a logarithmic singularity (this is dealt with in the future paper); when -2ϑ is not an integer, the coefficient of a_{n+1} in (5.1) never vanishes, leading to the recurrence relations

$$(n+1)(n+1\pm 2\vartheta)a^{\pm}_{n+1} = \{(n\pm 2\vartheta)(n-2)\pm 2\vartheta+2\Lambda^2\}a^{\pm}_n - 3\Lambda^2 a^{\pm}_{n-1} + \Lambda^2 a^{\pm}_{n-2}, \quad (5.2)$$

where the upper sign applies for $\sigma=0$, and the lower sign for $\sigma=-2\vartheta$. Since $a^{\pm}_0\neq 0$ is arbitrary, it can be incorporated in the arbitrary constants of integration $C_{\pm}$ in (3.20 *a*), i.e. one may set $a^{\pm}_0=1$. The next coefficients are given by

$$(1\pm 2\vartheta)a^{\pm}_1 = 2(\Lambda^2\mp\vartheta), \quad (5.3\,a)$$

$$4(1\pm\vartheta)a^{\pm}_2 = (2\Lambda^2-1)a^{\pm}_1 - 3\Lambda^2, \quad (5.3\,b)$$

$$3(3\pm 2\vartheta)a^{\pm}_3 = 2(\Lambda^2\pm\vartheta)a^{\pm}_2 - 3\Lambda^2 a^{\pm}_1 + \Lambda^2, \quad (5.3\,c)$$

and the remaining coefficients $a^{\pm}_n$, with $n=4,5,\ldots$, follow from (5.2).

Substituting (2.23) with $\sigma=0,-2\vartheta$ in (2.17 *a*), (2.14 *b*) specifies the linearly independent particular integrals

$$P_{\pm}(y;k,\omega) = \mathrm{e}^{\mp\vartheta y/L}\sum_{n=0}^{\infty} a^{\pm}_n\left\{\frac{\mathrm{e}^{-y/L}}{1-\Omega}\right\}^n, \quad (5.4)$$

whose linear combination (3.20 *a*) is the general integral of the wave equation (2.13) for the range of values of y indicated in (4.11). For the purposes of plotting, the distance from the wall y is normalized to the boundary-layer thickness L, namely

$$Y \equiv y/L, \quad (5.5\,a)$$

$$P_{\pm}(Y) \equiv P_{\pm}(y;k,\omega), \quad (5.5\,b)$$

and the wave fields are given by

$$P_{\pm}(Y) = \mathrm{e}^{\mp\vartheta Y}\left\{1+\sum_{n=1}^{\infty} a^{\pm}_n(1-\Omega)^{-n}\mathrm{e}^{-nY}\right\}, \quad (5.6)$$

which converge in the whole flow region flow $0<Y<\infty$ for $\Omega>2$ in (4.11). When $\Omega<\Omega_*$ in (2.30), then ϑ is real in (2.19 *b*), and only one solution is bounded as

$y \to \infty$, namely $P_-(Y)$, which represents surface waves, since

$$\Omega < 1 + \frac{1}{M}, \quad \lim_{Y \to \infty} P_-(Y) = 0. \tag{5.7}$$

In the opposite case σ is imaginary, and if $\sigma = \mathrm{i}|\sigma|$ then P_+ is an upward and P_- a downward propagating wave, and the solutions are complex conjugates:

$$\Omega > 1 + \frac{1}{M}, \quad P_+(Y) = P_-^*(Y) \equiv P(Y); \tag{5.8}$$

for example, standing modes can be obtained by setting $C_+ = C_-$ in (3.20 *a*):

$$C_+ = C_-, \quad P(y; k, \omega) = 2C_+ \operatorname{Re}\{P(Y)\}. \tag{5.9}$$

In the case (5.7) of surface waves, the plot concerns the logarithm of the acoustic pressure normalized to the value at the wall

$$Q(Y) = \log\{P_-(Y)/P_-(0)\}, \quad 0 \leqslant Y \leqslant 5, \tag{5.10}$$

versus distance from the wall, for five shear-layer thicknesses. In the case (5.8) of propagating waves,

$$Q_\pm(Y) = \log\{P_\pm(Y)/P_\pm(0)\} = \log|P_\pm(Y)/P_\pm(0)| + \mathrm{i}\{\arg P_\pm(Y) - \arg P_\pm(0)\}, \tag{5.11}$$

there are separate plots for the real part, which is the logarithm of the ratio of amplitudes, and the imaginary part, which is the phase difference between an arbitrary position and the wall.

The three independent parameters in the present problem are the dimensionless frequency Ω (2.12 *b*) and wavenumber K (2.16 *b*) and the Mach number (2.29):

$$\Lambda = (\Omega - 1)MK, \tag{5.12 a}$$

$$\vartheta = K\sqrt{1 - (\Omega - 1)^2 M^2}, \tag{5.12 b}$$

and all other parameters, e.g. Λ (2.16 *a*) and ϑ (2.19 *b*) are expressible in terms of these (5.12). The reference case is taken as the following values of the three parameters:

$$K = 5, \tag{5.13 a}$$

$$\Omega = 5, \tag{5.13 b}$$

$$M = 0.25, \tag{5.13 c}$$

namely (i) a compactness $5 = K = kL = 2\pi L/\lambda$ such that the horizontal wavelength $\lambda/L = \frac{2}{5}\pi = 1.257$ is of the order of the thickness of the boundary layer; (ii) a frequency $\Omega = 5$ for which there is no critical layer $\Omega > 1$ and the solution (5.6) converges $\Omega > 2$ over the whole flow region; and (iii) a low Mach number such that $\vartheta = 0$ in (5.12 *b*), corresponding to the borderline between oscillatory and evanescent sound fields in the free stream. Each of the parameters is next varied in turn, starting with the compactness:

$$\Omega = 5, \quad M = 0.25, \quad K = 1, 5, 10 \tag{5.14}$$

(as shown in figure 5). The logarithm of the sound field tends to a constant value in the free stream, regardless of the value of K, because $(\Omega - 1)M = 1$ and thus $\vartheta = 0$ in (5.12 *b*), corresponding to the borderline between asymptotically evanescent and oscillatory modes. The sound field does not vary much over the thickness of the

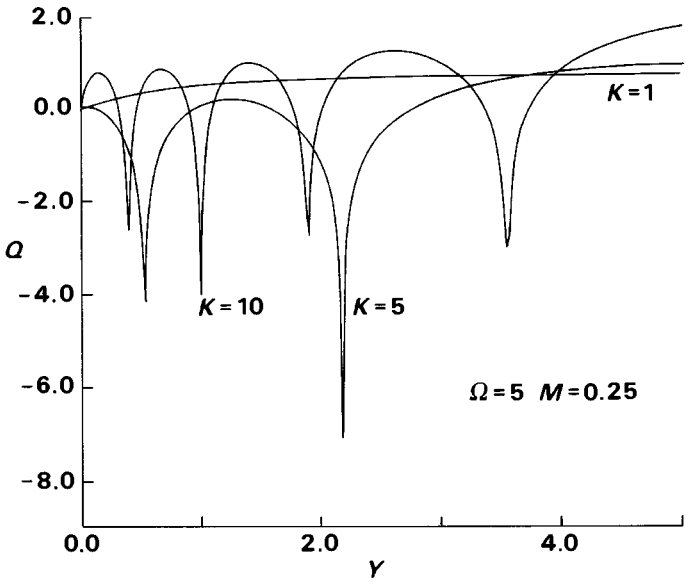

Figure 5. Logarithm of the acoustic pressure normalized to the wall value (5.10) versus dimensionless distance from the wall (5.5 *a*) for a surface wave. The dimensionless frequency and Mach number are fixed, and three dimensionless wavenumbers are considered.

boundary layer, the change between the wall and the free stream being a modest increase for large values of compactness. Significant sound level changes occur only at the zeros of the mode shape function, which are more closely spaced for larger K. In the case $K = 1$ there are no zeros of the mode shape function, because it is monotonic or evanescent, and the acoustic field is nearly uniform. In the case $K = 5$ there are two zeros, in the range of distances from the wall, and a very small amplitude increase towards the free stream. In the case $K = 10$ two more zeros, for a total of four, appear in the same range, and the amplitude increase towards the free stream is comparatively larger than before, but still small in absolute terms. Clearly, for larger wavenumbers, the zeros or nodes of the mode shape function are more closely spaced, on the scale of the thickness of the boundary layer.

The exponential rate of decay of the evanescent acoustic field in the free stream is determined by $\vartheta^2 < 0$ in (5.12 *b*), and increases for increasing frequency, as shown in figure 6, where the values

$$K = 5, \quad M = 0.25, \quad \Omega = 2, 3, 4 \tag{5.15}$$

are taken, namely the last below (5.13 *b*). The logarithm of the ratio of amplitudes decays linearly in the free stream, corresponding to the leading asymptotic term $\log P_+ \sim \vartheta Y$ in (5.6); therefore, for a given acoustic pressure at the wall, the acoustic field is smaller in the free stream as the frequency increases. Since in figure 6 the frequency has been reduced relative to (5.13 *b*), there are evanescent waves; if instead the frequency is increased,

$$K = 5, \quad M = 0.25, \quad \Omega = 5, 7, 10, \tag{5.16}$$

there are oscillatory waves in the free stream, needing separate plots for the logarithm of the ratio of amplitudes (difference of phases) in figure 7*a* (figure 7*b*). The amplitude

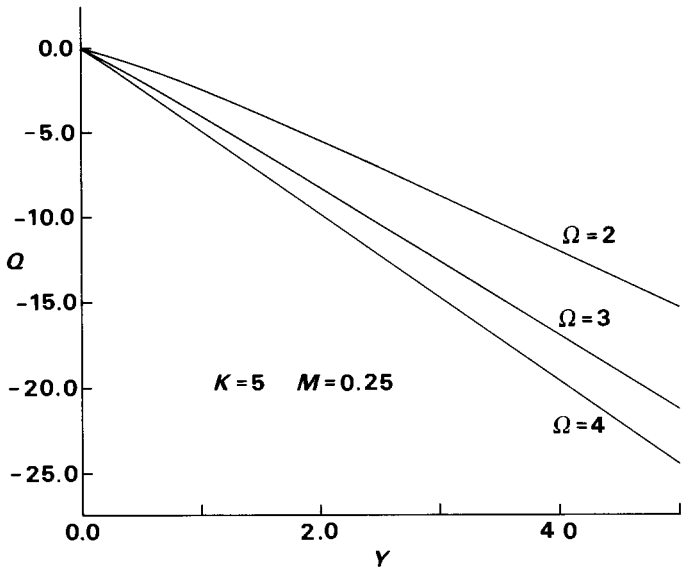

Figure 6. As figure 5, but with smaller frequency.

(figure 7*a*) is nearly constant and there are no zeros of the mode shape function for frequencies higher than the reference value $\Omega = 5$; the phase increases with distance almost linearly, and faster for a higher frequency, e.g. the slope is larger for $\Omega = 10$ than for $\Omega = 7$ (figure 7*b*). These are propagating waves, and in the borderline case $\Omega = 5$ to evanescent modes, the situation is quite different: (i) there are two zeros of the mode shape function, and a modest increase in amplitude in the free stream compared with the wall (figure 7*a*), as shown before (figure 5); (ii) there are no phase changes, since the mode is evanescent, except for phase jumps of $\pm\pi$ rad or $\pm 180^\circ$ corresponding to changes of sign across the zeros or nodes, leading to (figure 7*b*) a constant phase π between the two nodes, and a zero phase before the first, and after the second $\pi - \pi = 0$. Proceeding to the effects of the free-stream velocity, since in the case of non-homentropic mean flow the present theory is restricted to low Mach numbers, $M^2 \ll 1$, the values

$$K = 5 = \Omega, \quad M = 0.1, 0.2, 0.3, \tag{5.17}$$

are chosen for illustration in figure 8. Again there are surface waves, with amplitude decay away from the wall, the effect being smaller as the Mach number decreases. For homentropic mean flow the theory could be applied to an arbitrary Mach number.

6. Absorption at the critical layer

The next pair of solutions, in the neighbourhood of the critical layer, is specified by the differential equation (3.2), in terms of the variable

$$\xi = 1 - \frac{\mathrm{e}^{-y/L}}{1 - \Omega} = 1 - \exp\left\{\frac{y_\mathrm{c} - y}{L}\right\}, \tag{6.1}$$

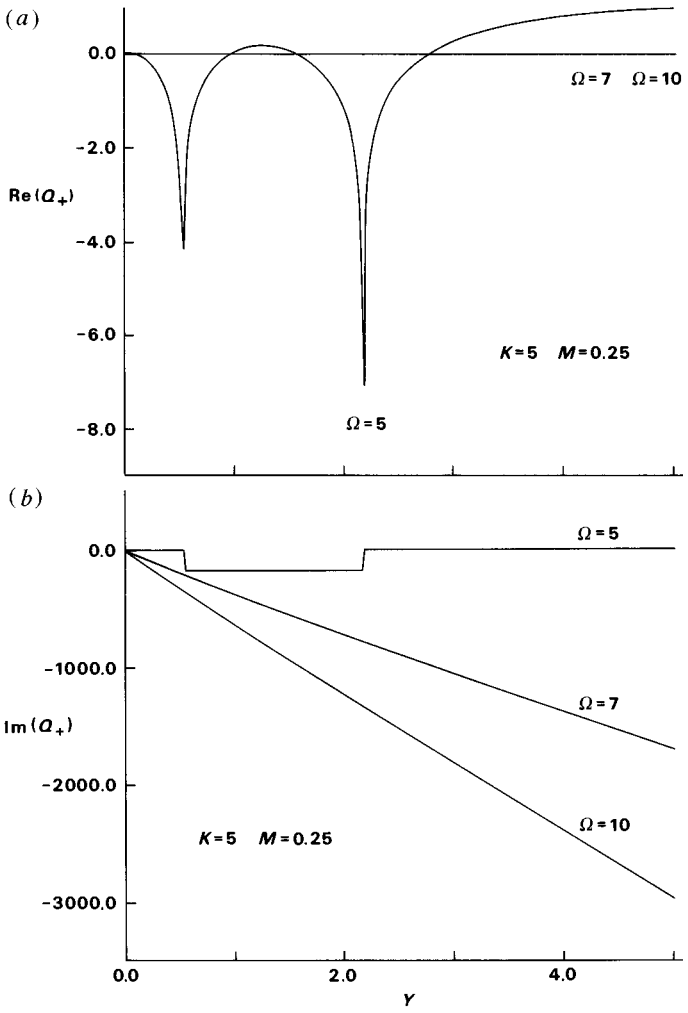

Figure 7. As figure 5, but with increased frequency, implying propagating waves, for which (5.11) the logarithm of the amplitude, normalized to the wall value, is shown in (*a*), and the phase shift relative to the wall value is shown (in degrees) in (*b*).

where use was made of (3.1 *a*), (2.14 *a*), (2.12 *a*). The substitution of the power series solution (3.5) leads to the recurrence formula

$$(n+\sigma+1)(n+\sigma-2)b_{n+1} = \{(n+\sigma)(n+\sigma-2\vartheta)-2\vartheta\}b_n + \Lambda^2(b_{n-1}+b_{n-2}) \tag{6.2}$$

for the coefficients. Setting $n=-1$ yields the indicial equation (3.6), which has roots $\sigma = 0, 3$, differing by an integer. The highest root $\sigma = 3$, gives rise to the solution

$$h_1(\xi) = \xi^3 \sum_{n=0}^{\infty} b_n(3)\xi^n, \tag{6.3}$$

where the coefficients of b_{n+1} in

$$(n+4)(n+1)b_{n+1} = \{(n+3)(n+3-2\vartheta)-2\vartheta\}b_n + \Lambda^2(b_{n-1}+b_{n-2}) \tag{6.4}$$

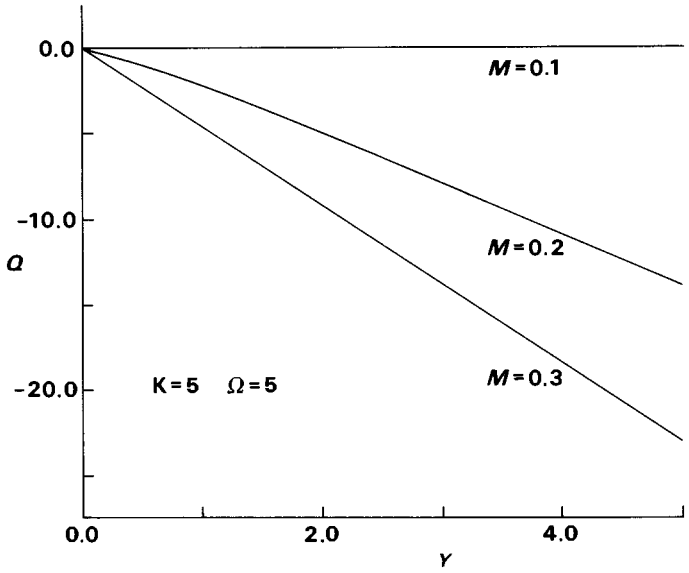

Figure 8. As figure 5, with reduced free-stream Mach number.

never vanish, e.g.

$$4b_1 = 9 - 8\vartheta, \tag{6.5a}$$

$$10b_2 = (16 - 10\vartheta)b_1 + \Lambda^2, \tag{6.5b}$$

$$18b_3 = (25 - 12\vartheta)b_2 + \Lambda^2 b_1 + \Lambda^2, \tag{6.5c}$$

where b_0 was set to unity $b_0 = 1$ because it can be incorporated in the arbitrary constant c_1 in (3.19 *a*). The lowest root $\sigma = 0$ gives rise to a solution with a logarithmic singularity, of which the leading term was considered previously (3.8); this solution can be obtained by the Frobenius–Fuchs method (further details will appear in a future paper).

The first plots concern the solution which vanishes at the critical layer, namely (2.14 *b*), (2.17 *a*), (3.1 *b*), (3.5), (6.1)

$$P_1(y;k,\omega) = \mathrm{e}^{-\vartheta y/L}\sum_{n=0}^{\infty} b_n\left\{1 - \frac{\mathrm{e}^{-y/L}}{1-\Omega}\right\}^{n+3}. \tag{6.6}$$

It is convenient to introduce the location of the critical layer in dimensionless form:

$$Y_\mathrm{c} \equiv y_\mathrm{c}/L = -\log(1-\Omega), \quad P_1(Y) = P_1(y;k,\omega), \tag{6.7}$$

so that the acoustic pressure is given by

$$P_1(Y) = \mathrm{e}^{-\vartheta Y}\sum_{n=0}^{\infty} b_n\left\{1 - \frac{\mathrm{e}^{-Y}}{1-\Omega}\right\}^{n+3} = \mathrm{e}^{-\vartheta Y}\sum_{n=0}^{\infty} b_n(1-\mathrm{e}^{Y_\mathrm{c}-Y})^{n+3}. \tag{6.8}$$

The value at the wall (6.9 *a*)

$$P_1(0) = \sum_{n=0}^{\infty} b_n\left(1 - \frac{1}{\Omega}\right)^{-n-3}, \tag{6.9a}$$

$$Q_1(Y) = \log\left\{\frac{P_1(Y)}{P_1(0)}\right\}, \tag{6.9b}$$

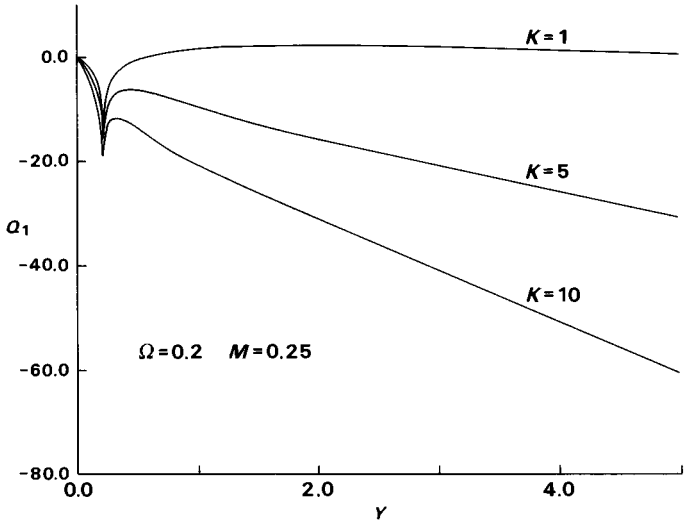

Figure 9. As for figure 5, using solution vanishing at the critical layer, and a much smaller fixed frequency: the same low Mach number, and three values of wavenumber.

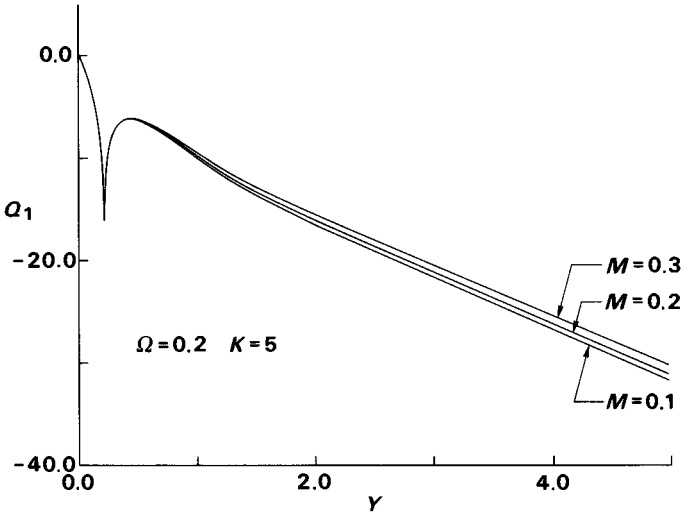

Figure 10. As figure 9, changing the Mach number.

is used for normalization (6.9 *b*) in figures 9–12. In the case $\Omega < \frac{1}{2}$, this solution covers the whole flow region, because condition (3.19 *b*) is met for all $0 < y < \infty$, as indicated in (4.11).

The reference case is taken for the same values of dimensionless wavenumber and Mach number as before (5.13 *a*), (5.13 *c*):

$$K = 5, \quad \Omega = 0.2, \quad M = 0.25, \tag{6.10}$$

with a much smaller dimensionless frequency, in the range $|\Omega - 1|M = 0.2 < 1$ of surface waves. The effect of changing values of wavenumber is shown in figure 9:

$$K = 1, 5, 10, \quad \Omega = 0.2, \quad M = 0.25. \tag{6.11}$$

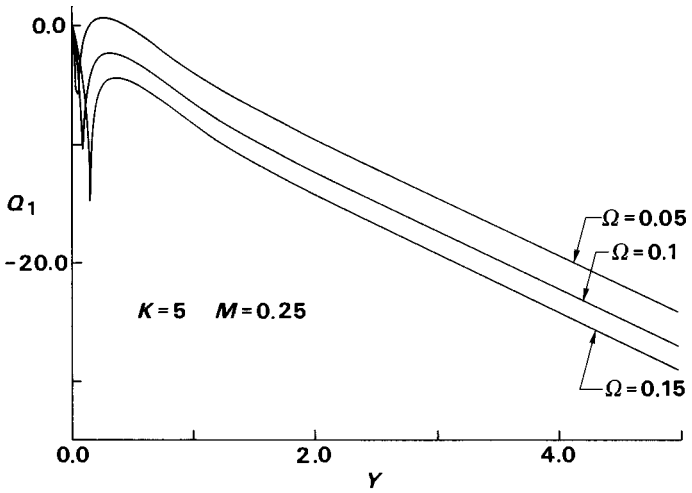

Figure 11. As figure 9, reducing the frequency.

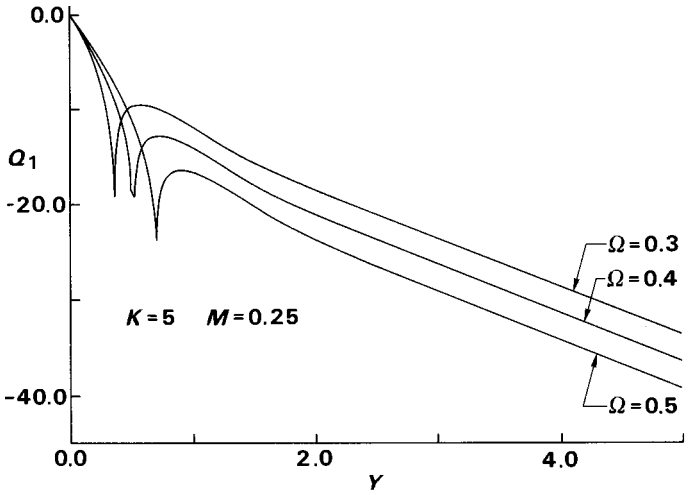

Figure 12. As figure 9, increasing the frequency.

The zero of the mode shape function occurs always at the same position, since the location of the critical layer (2.12 a) is unaffected by the wavenumber; as the latter increases the acoustic pressure decays away from the wall with a larger slope. In figure 10 the effect of free-stream Mach number

$$K = 5, \quad \Omega = 0.2, \quad M = 0.1, 0.2, 0.3 \tag{6.12}$$

always in the low Mach number range, is shown to be small with regard to the amplitude decay away from the wall; it does not affect the location of the zero of the mode shape function. The latter depends only on the dimensionless frequency, which is decreased in figure 11:

$$K = 5, \quad \Omega = 0.05, 0.10, 0.15, \quad M = 0.25, \tag{6.13}$$

and increased in figure 12:

$$K = 5, \quad \Omega = 0.3, 0.4, 0.5, \quad M = 0.25, \tag{6.14}$$

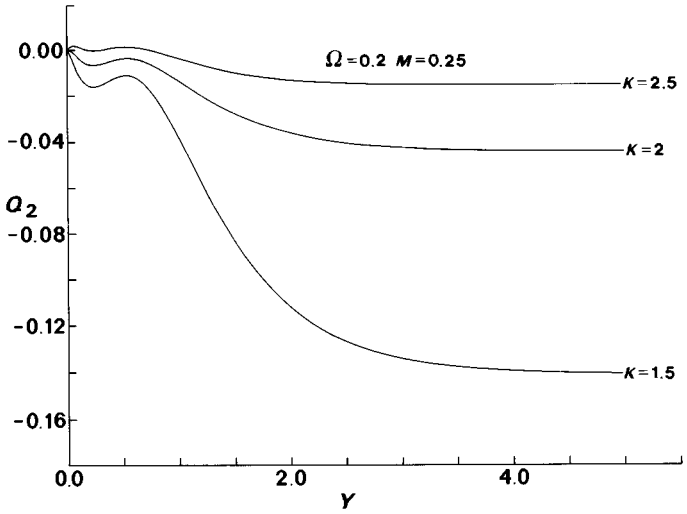

Figure 13. As figure 5, for solution which is finite at the critical layer. Same low frequency as in figure 9; Mach number also fixed. Three values of wavenumber considered.

while remaining within $\Omega \leqslant \frac{1}{2}$. In both cases, as frequency increases, the zero of the mode shape function moves away from the wall. The amplitude decay away from the wall has a similar slope for all frequencies, but the absolute value at each position decreases as frequency increases.

The other solution in the neighbourhood of the critical layer involves a logarithmic singularity, as is documented elsewhere, e.g. for internal (Booker & Bretherton 1966), instability (Drazin & Reid 1981) and hydromagnetic (Eltayeb 1977) waves. The reference case taken is

$$K = 2, \quad \Omega = 0.2, \quad M = 0.25, \tag{6.15}$$

for the solution (3.8), with logarithmic singularity at the critical level $\log \xi$ dominated by the triple zero ξ^3, so that $P_2 \sim 0(1)$ is finite there. The plots concern the logarithm of the ratio of amplitude at position Y to the amplitude at the wall:

$$Q_2(Y) = \log\left\{\frac{P_2(Y;k,\omega)}{P_2(0;k,\omega)}\right\}, \tag{6.16}$$

versus the dimensionless distance from the wall $(5.5\,a)$. The wavenumber is varied first:

$$K = 1.5, 2, 2.5, \quad \Omega = 0.2, \quad M = 0.25, \tag{6.17}$$

in figure 13, showing that the amplitude tends, in the free stream, to a constant asymptotic value, which is lower for a smaller wavenumber. The amplitude plot is not a monotonic function of distance, since there is a local maximum at the critical layer. Towards the free stream there are no more local maxima, i.e. just a decay, which is more pronounced for a smaller wavenumber. The local maximum at the critical layer is higher than the value at the wall for $K = 2.5$ and smaller for $K = 2, 1.5$, and in all cases there is a local minimum in between. In the case $K = 2.5$ there is a further local maximum, between the local minimum and the wall, because the amplitude initially increases away from the wall. Next the Mach number is given the

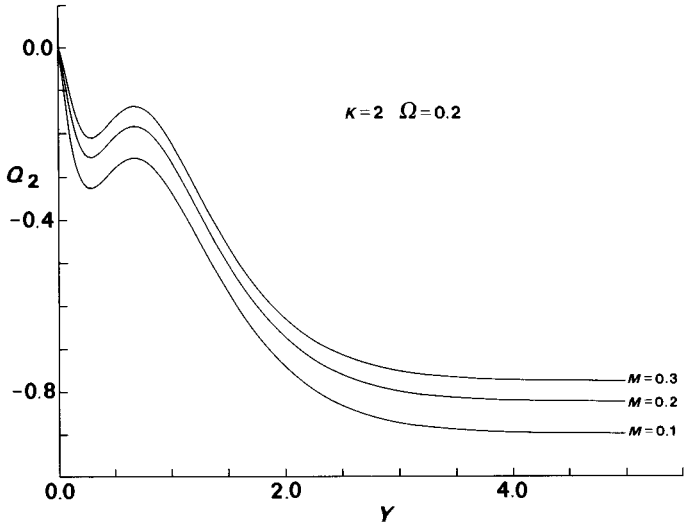

Figure 14. As figure 13, changing the Mach number.

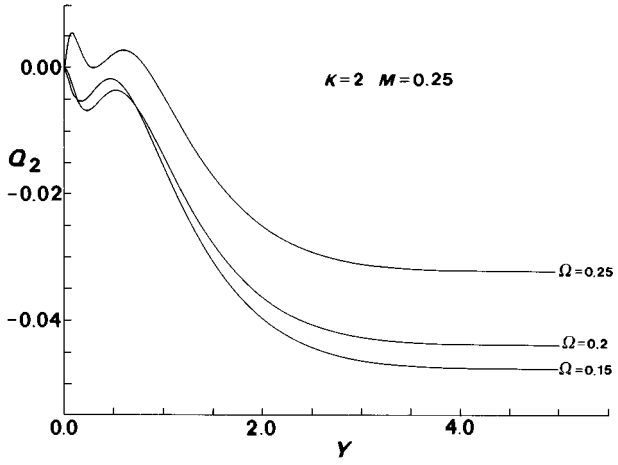

Figure 15. As figure 14, reducing the frequency.

values

$$K = 2, \quad \Omega = 0.2, \quad M = 0.1, 0.2, 0.3, \tag{6.18}$$

showing in figure 14 that the amplitude is slightly smaller for a lower Mach number, but follows a similar evolution, starting with decay away from the wall, followed by increase towards the local maximum at the critical layer, and a final decay towards a constant asymptotic value in the free stream. Varying the frequency,

$$K = 2, \quad \Omega = 0.15, 0.2, 0.25, \quad M = 0.25, \tag{6.19}$$

as shown in figure 15, has a broadly similar effect to varying wavenumber (in figure 13), except that the amplitudes for lower frequencies can cross, while still tending to a constant asymptotic amplitude in the free stream, which is smaller for a lower frequency.

7. Rigid or impedance walls

In general, the wave field satisfying a pair of independent and compatible boundary conditions is a linear combination of pairs of solutions of the type considered before; namely outward P_+ or inward P_- propagating waves in the free stream, vanishing P_1 or finite P_2 waves near the critical layer, or the wave fields P_* and P_{**} below the critical layer; in some cases, in order to obtain the wave field over the whole flow region, analytic continuation between pairs of solutions may be necessary (4.11), e.g. across the critical layer. In the particular case when the critical layer lies in the free stream, only one pair of solutions is needed; the reason is that two of the three singularities of the wave equation coincide, so that only two singularities are left, one at the origin and one at infinity, and the radius of convergence is infinite. In all these cases, the question arises of the determination of the constants of integration, specifying the linear combination of two particular solutions, which satisfies a given pair of compatible and independent boundary conditions. Thus, rather than plotting more of the pairs of particular integrals ($P_\pm, P_{1,2}$ and $P_{*,**}$) which, by linear combination and analytic continuation, form general solutions, one may proceed to illustrate the determination of the constants of integration. This can be done for any case, e.g. when a critical layer does not exist, and a linear combination (3.20 *a*) of outward P_+ and inward P_- propagating waves, specifies the sound field over the whole flow region:

$$P(Y) = C_+ P_+(Y) + C_- P_-(Y), \tag{7.1}$$

with $P_\pm(Y)$ given by (5.6). The boundary conditions taken are a given wave amplitude at the free stream (7.2 *a*),

$$P(Y=\infty) = P_\infty, \tag{7.2\,a}$$

$$\left.\frac{\mathrm{d}P}{\mathrm{d}Y}\right|_{Y=0} = \mathrm{i}\rho\omega(L/Z)P(0), \tag{7.2\,b}$$

and an impedance boundary condition (4.2 *b*) at the wall (7.2 *b*). The latter condition (7.2 *b*) can be written in terms of dimensionless parameters (7.3 *a*):

$$P'(0) = \mathrm{i}(\Omega K M/\bar{Z})P(0), \tag{7.3\,a}$$

$$\bar{Z} \equiv Z/\rho c, \tag{7.3\,b}$$

where use was made of the dimensionless frequency (2.12 *b*), wavenumber (2.16 *b*), besides the Mach number (2.29) and dimensionless or specific impedance (7.3 *b*). The case of a rigid wall $\bar{Z} = \infty$, and sound of constant amplitude in the free stream, leads to

$$P(\infty) = P_\infty, \quad P(0) = 0 \tag{7.4}$$

as boundary conditions.

Substituting these boundary conditions in (7.1), together with (5.6) and

$$P'_\pm(Y) = \mathrm{e}^{\mp\vartheta Y}\left\{\mp\vartheta + \sum_{n=1}^{\infty}(-n \mp \vartheta)a_n^\pm(1-\Omega)^{-n}\mathrm{e}^{-nY}\right\}, \tag{7.5}$$

implies that the coefficients $C_\pm$ are specified by the linear inhomogeneous system of equations

$$\begin{bmatrix} P_+(\infty) & P_-(\infty) \\ P'_+(0) - \mathrm{i}(\Omega M K/\bar{Z})P_+(0) & P'_-(0) - \mathrm{i}(\Omega M K/\bar{Z})P_-(0) \end{bmatrix} \begin{bmatrix} C_+ \\ C_- \end{bmatrix} = \begin{bmatrix} P_\infty \\ 0 \end{bmatrix} \tag{7.6}$$

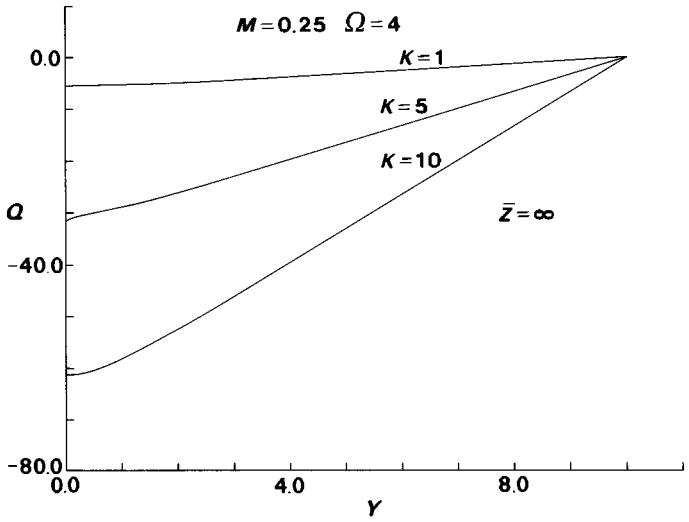

Figure 16. Logarithm of acoustic pressure, normalized to the value at $Y = 10$, versus dimensionless distance from a *rigid* wall. Fixed frequency and Mach number, and three values of wavenumber.

for an impedance wall, simplifying to

$$\bar{Z} = \infty, \quad \begin{bmatrix} P_+(\infty) & P_-(\infty) \\ P'_+(0) & P'_-(0) \end{bmatrix} \begin{bmatrix} C_+ \\ C_- \end{bmatrix} = \begin{bmatrix} P_\infty \\ 0 \end{bmatrix} \tag{7.7}$$

for a rigid wall. For practical purposes the free stream $Y = \infty$ is replaced by $Y = 10$, and this determines the range of distances from the wall (7.8 *a*):

$$0 \leqslant Y \leqslant 10, \tag{7.8 a}$$

$$Q(Y) \equiv \log\left\{\frac{P(Y)}{P_\infty}\right\}, \tag{7.8 b}$$

over which is plotted the sound field normalized to the value in the free stream (7.8 *b*). Thus figures 5–15 contain plots of sound-field 'components', and figures 16–23 show plots of the total wave field, which is their linear combination. For propagating waves, the real and imaginary parts of (7.8 *b*) are plotted separately, corresponding, respectively, to the logarithm of the ratio of amplitudes at position Y and the free stream (7.9 *a*):

$$\mathrm{Re}(Q) = \log|P(Y)/P_\infty|, \tag{7.9 a}$$

$$\mathrm{Im}(Q) = \arg(P) - \arg(P_\infty), \tag{7.9 b}$$

and the phase shift (7.9 *b*) between the free stream and position Y.

The first set of plots (figures 16–19) concerns a rigid wall, and takes as the baseline case

$$\bar{Z} = \infty, \quad K = 1, \quad \Omega = 4, \quad M = 0.25. \tag{7.10}$$

Varying first the wavenumber,

$$\bar{Z} = \infty, \quad K = 1, 5, 10, \quad \Omega = 4, \quad M = 0.25, \tag{7.11}$$

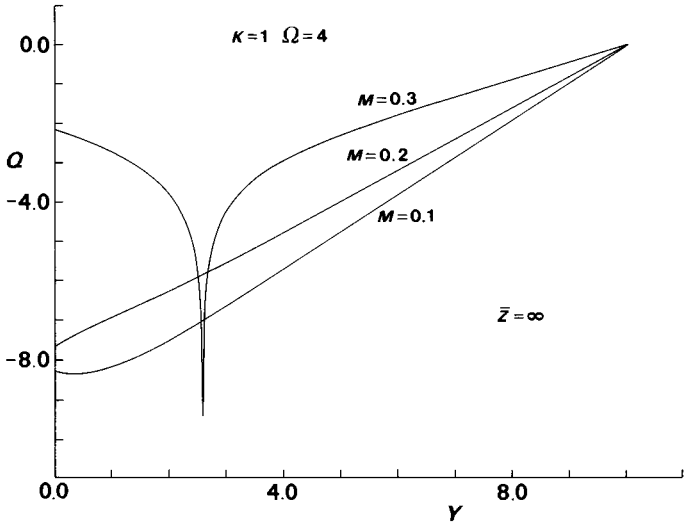

Figure 17. As figure 16, for three values of Mach number.

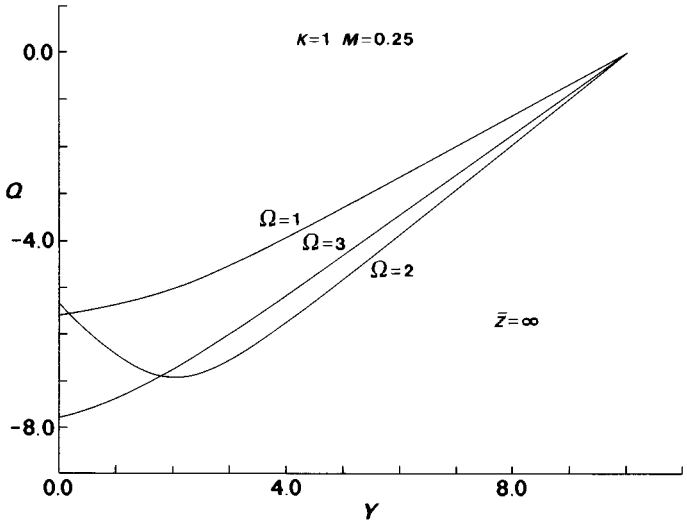

Figure 18. As figure 16, reducing the frequency.

shows (figure 16) that the amplitude decays faster towards the wall for a larger wavenumber. Varying the Mach number,

$$\bar{Z} = \infty, \quad K = 1, \quad \Omega = 4, \quad M = 0.1, 0.2, 0.3, \tag{7.12}$$

shows (figure 17) a faster decay of amplitude towards the wall, for a smaller Mach number; a zero of the mode shape function occurs in the range (7.8 *a*) for $M = 0.3$, but not for lower values $M = 0.1, 0.2$. Reducing the frequency,

$$\bar{Z} = \infty, \quad K = 1, \quad \Omega = 2, 3, 4, \quad M = 0.25, \tag{7.13}$$

leads (figure 18) to a faster decay of amplitude away from the free stream, towards the wall; for low frequencies the curves are not monotonic, and an increase in amplitude

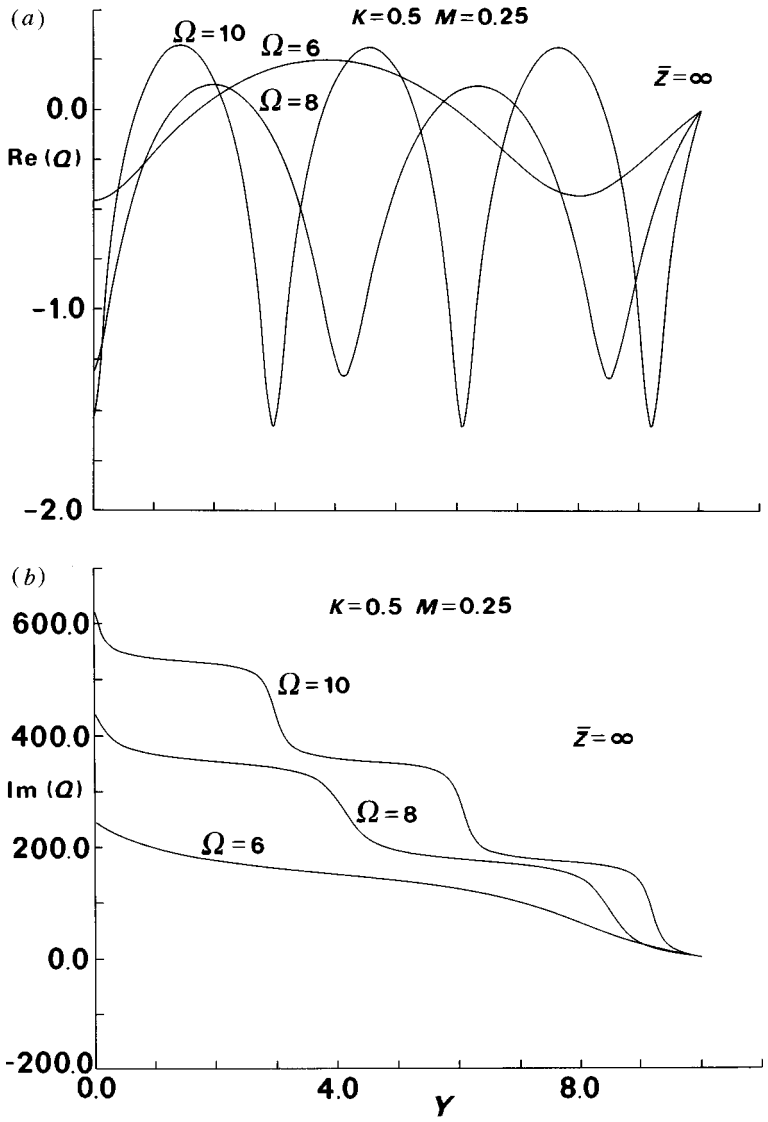

Figure 19. As figure 16, with increased frequency, leading to propagating waves, with logarithm of the amplitude, normalized to value at free stream in (*a*), and phase shift from free stream in (*b*).

near the wall can be observed for $\Omega = 2$. For $M = 0.25$ there are surface (or non-propagating) waves, for real ϑ in (5.12 *b*), i.e. all the plots in figures 16–18. If the frequency is increased,

$$\bar{Z} = \infty, \quad K = 1, \quad \Omega = 6, 8, 10, \quad M = 0.25, \tag{7.14}$$

there are propagating waves, whose amplitudes (figure 19*a*) have larger variations for larger frequencies; the zeros of the mode shape functions correspond (figure 19*b*) to 180° (or π rad) phase jumps, otherwise the phase varies little, in the 'plateaux'

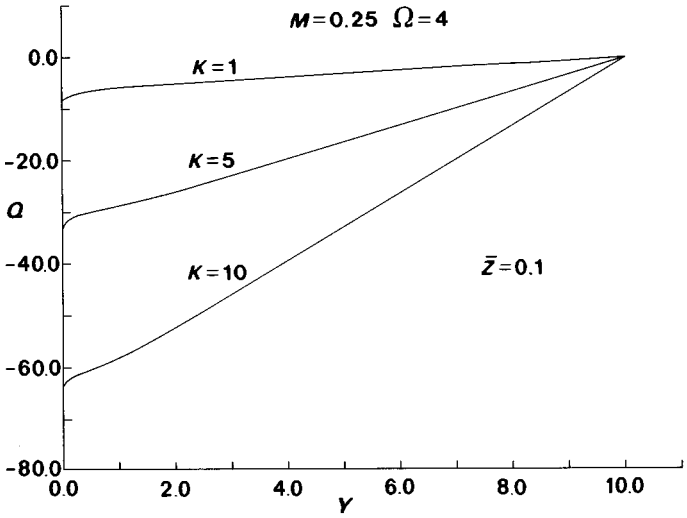

Figure 20. As figure 16, replacing rigid wall by impedance wall.

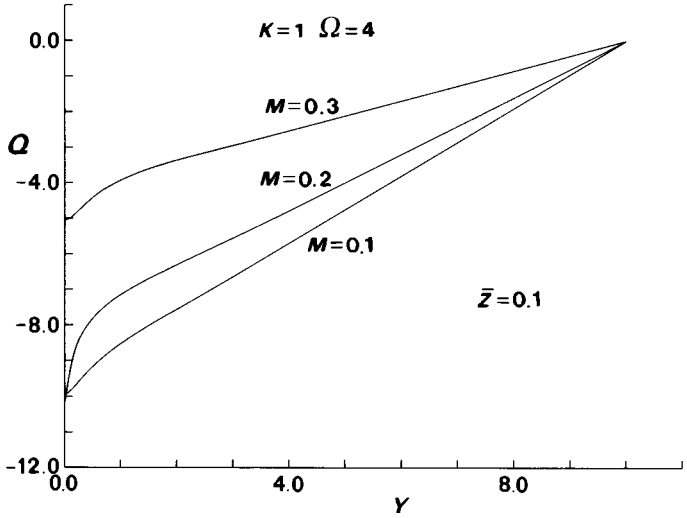

Figure 21. As figure 17, replacing rigid wall by impedance wall.

between the phase jumps. Also the phase jumps in figure 19*b* are smoother than those in figure 7*b*.

Consider next an impedance wall, for the same baseline case (7.10) as before:

$$\bar{Z} = 0.1, \quad K = 1, \quad \Omega = 4, \quad M = 0.25. \tag{7.15}$$

Varying the wavenumber,

$$\bar{Z} = 0.1, \quad K = 1, 5, 10, \quad \Omega = 4, \quad M = 0.25, \tag{7.16}$$

shows that (figure 20) the amplitude decays from the free stream to the wall, faster for a larger wavenumber, with slightly smaller values at the wall than for the rigid wall (figure 16); the impedance wall causes an amplitude reduction in the last fraction of shear-layer thickness, namely the curvature of the amplitude curve near the wall

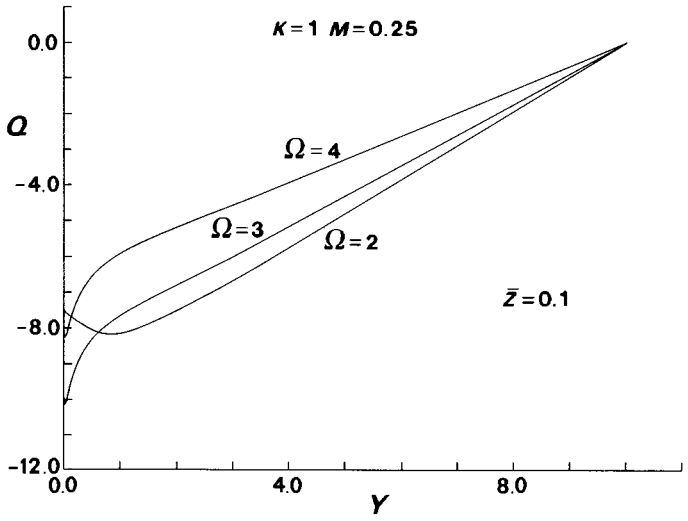

Figure 22. As figure 18, replacing rigid wall by impedance wall.

is positive for a rigid wall (figure 16) and negative for an impedance wall (figure 20). The effect of varying the Mach number,

$$\bar{Z} = 0.1, \quad K = 1, \quad \Omega = 4, \quad M = 0.1, 0.2, 0.3, \tag{7.17}$$

has a similar (figure 21) interpretation, with a smaller amplitude for a smaller Mach number. Reducing the frequency,

$$\bar{Z} = 0.1, \quad K = 1, \quad \Omega = 2, 3, 4, \quad M = 0.25, \tag{7.18}$$

shows (figure 22) (i) a faster decay of amplitude towards the wall for lower frequencies; (ii) an amplitude increase near the wall for low frequencies; (iii) an amplitude decrease very near the impedance wall relative to the rigid wall. Increasing the frequency,

$$\bar{Z} = 0.1, \quad K = 1, \quad \Omega = 6, 8, 10, \quad M = 0.25, \tag{7.19}$$

leads to propagating waves, which have larger amplitude fluctuations as the frequency increases (figure 23*a*), and also as impedance increases (cf. rigid wall in figure 19*a*). The phase jumps at the zeros of the mode shape functions are sharper, with flatter 'plateaux' in between for the impedance (figure 23*b*) relative to the rigid (figure 19*b*) wall.

8. Critical layer in the free stream

The process of linear combination of pairs of solutions to satisfy boundary conditions works equally well with or without the critical layer, whether or not one needs one, two or three pairs of solutions ($P_{\pm}, P_{1,2}$ and $P_{*,**}$) and their analytic continuation. In the case of a critical layer in the free stream, since two singularities coincide, only two singularities remain, and thus only one pair of solutions is needed. This pair of solutions is different from the preceding solutions, because the coalescence of two regular singularities (the critical layer and the free stream) leads to one regular singularity, leaving only one other singularity, which remains irregular. As is shown

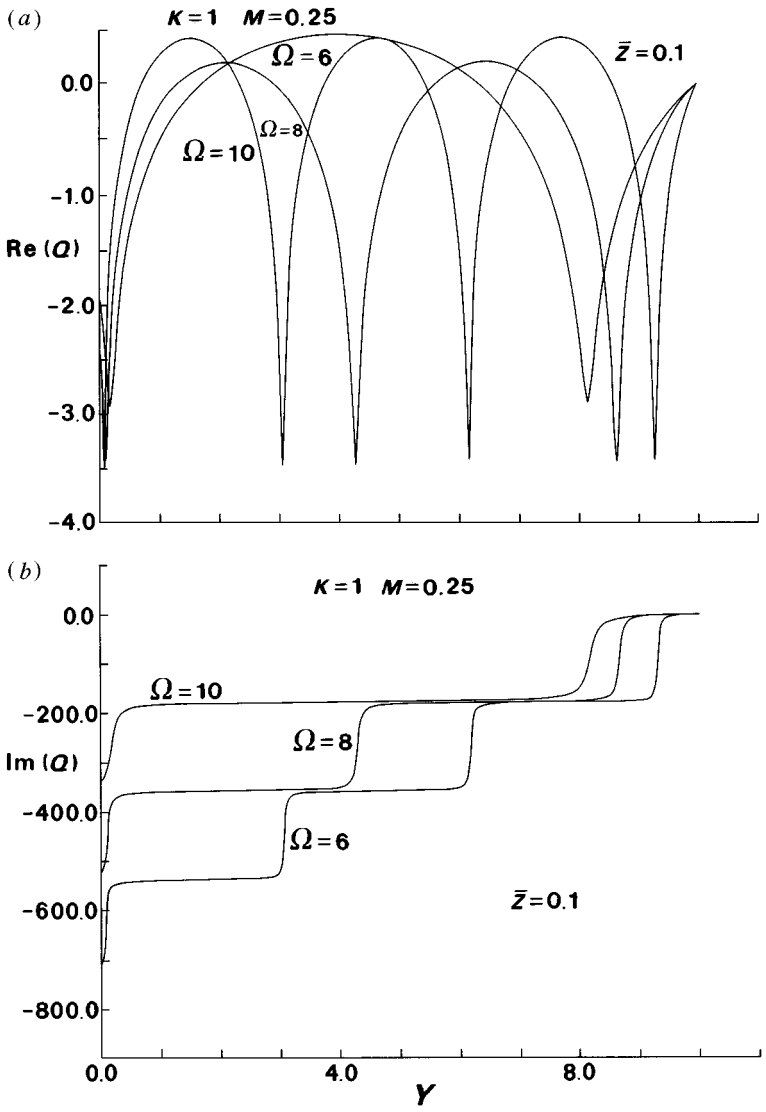

Figure 23. As figure 19, replacing rigid wall by impedance wall.

next, the solution is simpler in this particular case. The preceding discussion (in § 2 to § 7) does not apply when the critical layer lies in the free stream $\Omega = 1$, because in this case the variable $\zeta = \infty$ in (2.14 *a*), and all the variables in the Kleinian group (3.15) are zero or infinity. It turns out that this case is particularly simple, and all instances can be discussed briefly including those involving logarithmic and essential singularities (which are deferred to a future paper in the general case), because this is one of the many problems solvable in terms of Bessel functions (Watson 1944; Erdelyi 1953; Abramowitz & Stegun 1965; Luke 1975; Campos 1994; Campos & Gil 1995). When $\Omega = 1$, the general wave equation (2.13), simplifies to

$$P'' + (2/L)P' + (M^2 \mathrm{e}^{-2y/L} - 1)k^2 P = 0. \tag{8.1}$$

The change of independent variable,

$$\zeta = M\mathrm{e}^{-y/L}, \quad P(y;k,kV) = f(\zeta) \equiv R(y;K,KM), \tag{8.2}$$

places the critical layer in the free stream $y = \infty$ at the origin $\zeta = 0$, and transforms (8.1) to

$$\zeta^2 f'' - \zeta f' + (\zeta^2 - 1)K^2 f = 0, \tag{8.3}$$

which differs from a Bessel equation only in the sign of the coefficient of f'. The change of dependent variable (8.4),

$$f(\zeta) = \zeta g(\zeta), \tag{8.4}$$

leads to a Bessel equation

$$\zeta^2 g'' + \zeta g' + [K^2\zeta^2 - (1 + K^2)]g = 0, \tag{8.5}$$

of variable $K\zeta$ and order $\sqrt{1 + K^2}$, whose solution is

$$g(\zeta) = S_{\sqrt{1+K^2}}(K\zeta), \tag{8.6}$$

where S is a linear combination of linearly independent Bessel functions.

For example, in the exceptional case where the order is an integer $n = \sqrt{1 + K^2} \geqslant 1$, the solution is a linear combination of Bessel J_n and Neumann G_n functions of order n (Watson 1944):

$$n = \sqrt{1 + K^2}, \quad S_n(K\zeta) \equiv C_1 J_n(K\zeta) + C_2 G_n(K\zeta), \tag{8.7}$$

and the acoustic pressure is given by

$$R(y;\sqrt{n^2-1}, M\sqrt{n^2-1}) = \mathrm{e}^{-y/L}\{C_1 J_n(\sqrt{n^2-1}M\mathrm{e}^{-y/L}) + C_2 G_n(\sqrt{n^2-1}M\mathrm{e}^{-y/L})\}. \tag{8.8}$$

Near the free stream $y \gg L$, the variable is small, $\mathrm{e}^{-y/L}KM \ll 1$, and use of the approximations (Abramowitz & Stegun 1965)

$$\xi \equiv \zeta\sqrt{n^2-1}, \tag{8.9a}$$

$$J_n, G_n(\xi) = \{(\tfrac{1}{2}\xi)^n, -(1/\pi)(\tfrac{1}{2}\xi)^{-n}\}\{1 + O(\xi^2)\}, \tag{8.9b}$$

in the acoustic pressure shows that the sound field in the free stream is given by

$$R(y;\sqrt{n^2-1}, M\sqrt{n^2-1}) \sim \frac{C_2}{\pi}(\tfrac{1}{2}M\sqrt{n^2-1})^{-n}\mathrm{e}^{(n-1)y/L}. \tag{8.10}$$

Note that for n, the lowest positive integer $n = 1$, there is no longitudinal propagation $K = 0$, and for larger values $n = 2, 3, \ldots$, then $K > 0$ so that the waves are propagating; for large n,

$$n^2 \gg 1, \quad K = \sqrt{n^2-1} \sim n - 1/2n + O(n^{-3}) \tag{8.11}$$

corresponding to the ray limit $K^2 \gg 1$, the pressure field scales as

$$R(y,n,Mn) \sim \frac{C_2}{\pi}(\tfrac{1}{2}nM)^{-n}\mathrm{e}^{ny/L}. \tag{8.12}$$

Note that in the present case $\Omega = 1$ of the critical layer in the free stream, it follows from (5.12*b*) that $\vartheta = \pm K$; in the ray limit of large $K \sim n$, or $n = \mp\vartheta$, the acoustic pressure (8.12) agrees with (2.25).

In the general case, when the order is not an integer, the pressure field is a linear combination of Bessel functions of orders $\pm\sqrt{1+K^2}$, namely $(1+K^2 \neq n^2)$

$$P(y;k,kV) = \mathrm{e}^{-y/L}\{C_1 J_{\sqrt{1+K^2}}(KM\mathrm{e}^{-y/L}) + C_2 J_{-\sqrt{1+K^2}}(KM\mathrm{e}^{-y/L})\}. \quad (8.13)$$

Near the free stream the variable is small, and using (8.9 *a*), namely

$$\xi = K\zeta, \quad J_\vartheta(\xi) \sim (\tfrac{1}{2}\xi)^\vartheta\{1+O(\xi^2)\}, \quad (8.14)$$

yields

$$R(y;K,KM) \sim C_2(\tfrac{1}{2}KM)^{\sqrt{1+K^2}}\mathrm{e}^{(\sqrt{1+K^2}-1)y/L}. \quad (8.15)$$

In the ray limit $K^2 \gg 1$, this simplifies to

$$R(y;K,KM) \sim C_2(\tfrac{1}{2}KM)^K \mathrm{e}^{Ky/L}, \quad (8.16)$$

which again agrees with (8.12) and (2.25). Since the Bessel equation (8.5) has a regular singularity at $\zeta = 0$ in the free stream $y = +\infty$, and an irregular one $\zeta = \infty$ below the wall $y = -\infty$, the solutions in terms of Bessel (8.13), Neumann (8.8) and Hankel (8.17) functions,

$$R(y;K,KM) = \mathrm{e}^{-y/L}\{C_+ H^{(1)}_{\sqrt{1+K^2}}(KM\mathrm{e}^{-y/L}) + C_- H^{(2)}_{\sqrt{1+K^2}}(KM\mathrm{e}^{-y/L})\}, \quad (8.17)$$

have an infinite radius of convergence, and cover the whole flow region $0 < y < \infty$.

The plots concern the logarithm of the acoustic pressure normalized to the wall value:

$$W_{1,2}(Y) = \mathrm{e}^{-Y}\frac{H^{(1,2)}_{\sqrt{1+K^2}}(KM\mathrm{e}^{-Y})}{H^{(1,2)}_{\sqrt{1+K^2}}(KM)}, \quad (8.18\,a)$$

$$W(Y) \equiv \log\{W_1(Y)\}, \quad (8.18\,b)$$

versus distance from the wall, for five boundary-layer thicknesses $0 \leqslant Y \equiv y/L \leqslant 5$. The real (imaginary) part, i.e. the logarithm of amplitudes (phase difference) applies to both wave components

$$\mathrm{Re}(W) = \log|W_1| = \log|W_2|, \quad (8.19\,a)$$

$$\mathrm{Im}(W) = \arg(W_1) = -\arg(W_2), \quad (8.19\,b)$$

and is plotted on the tops of figures 24 and 25, respectively, for Mach numbers (8.20 *a*)

$$M = 0.15, 0.3, \quad (8.20\,a)$$

$$K = 0.5, 1, 2, 5, \quad (8.20\,b)$$

in each case for the same four values of wavenumber (8.20 *b*). For the lower Mach number (figure 24), the amplitude (*a*) decays exponentially towards the free stream, being smaller for a larger wavenumber; the increase of the latter corresponds to larger phase changes (*b*), which tend to a constant in the free stream. The same effects are observed (figure 25), in a more pronounced form, for higher Mach numbers, both as concerns amplitude (*a*) and phase (*b*).

Since the preceding solution is valid for $y < 0$, it can be used to investigate the properties of the acoustic pressure, in a region of increasing vorticity of the mean flow. For all values of K the result (8.17) in the asymptotic form

$$H^{(1,2)}_\nu(\xi) \sim \sqrt{\frac{2}{\pi\xi}}\exp\{\pm\mathrm{i}(\xi - \tfrac{1}{2}\nu\pi - \tfrac{1}{4}\pi)\}\{1+O(\xi^{-1})\} \quad (8.21)$$

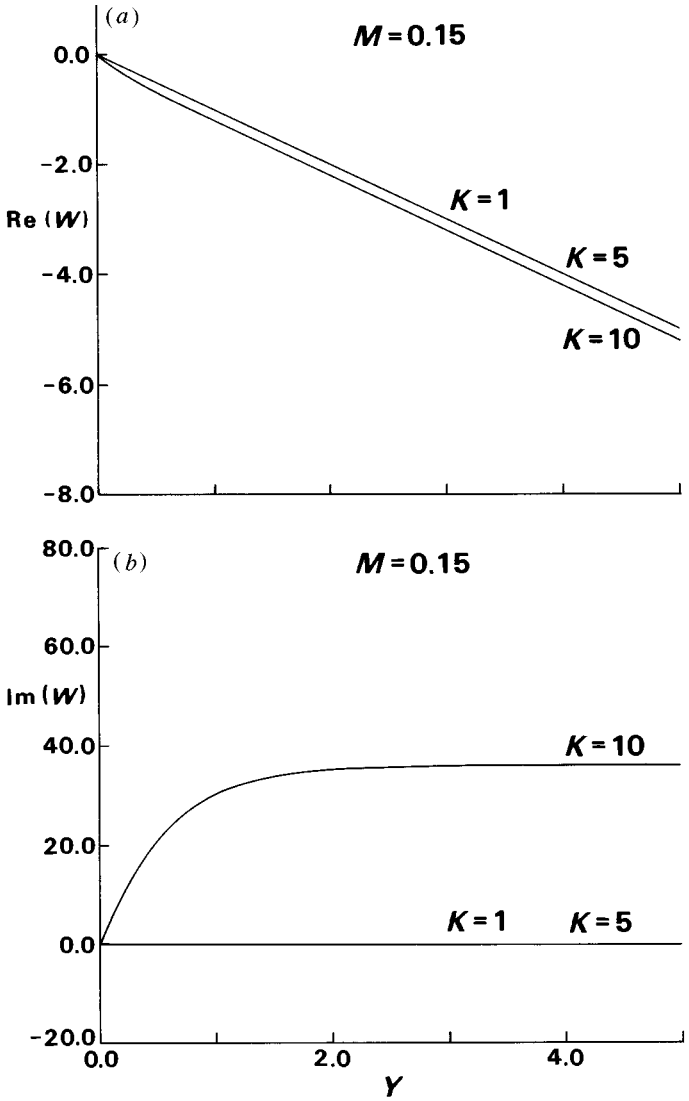

Figure 24. Logarithm of amplitude normalized to the wall (a) and phase shift relative to wall value (b), versus dimensionless distance from the wall, for acoustic pressure of an outward (inward) propagating wave, in the case of a critical layer at the free stream. Fixed Mach number and four values of wavenumber.

can be used to investigate the mathematical nature of the essential singularity of the solution

$$R(y;K,KM) \sim \mathrm{e}^{-y/2L} A \exp\{\pm \mathrm{i} KM \mathrm{e}^{-y/L} - B\}, \tag{8.22}$$

where

$$A \equiv C_{\pm}\sqrt{(2/\pi KM)}, \tag{8.23\,a}$$

$$B \equiv \tfrac{1}{2}\pi(\sqrt{1+K^2} - \tfrac{1}{2}). \tag{8.23\,b}$$

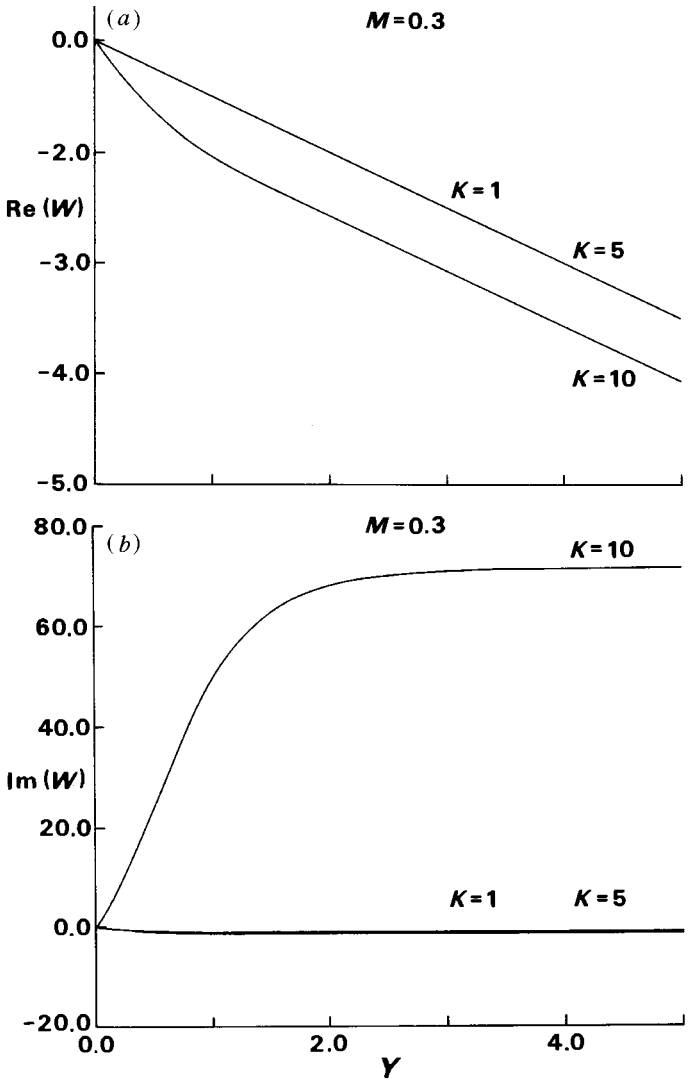

Figure 25. As figure 24, with same wavenumbers, and larger, but still low Mach number.

As $y \to -\infty$ the solution does indeed have an essential singularity:

$$R(y; K, KM) \sim A\mathrm{e}^{-B} \sum_{n=0}^{\infty} \{(\pm \mathrm{i}KM)^n / n!\} \mathrm{e}^{-(n+(1/2))y/L}, \tag{8.24}$$

because of the unbounded phase oscillation. The amplitude has a simple exponential form:

$$|R(y; K, KM)| \sim A \exp\left(-B - \frac{y}{2L}\right). \tag{8.25}$$

Another physical situation in whose connection an essential singularity occurs is sound propagation in a nozzle with power-law cross-section containing a low Mach number mean flow (Campos 1987*b*); in this case the vertex is outside the physical

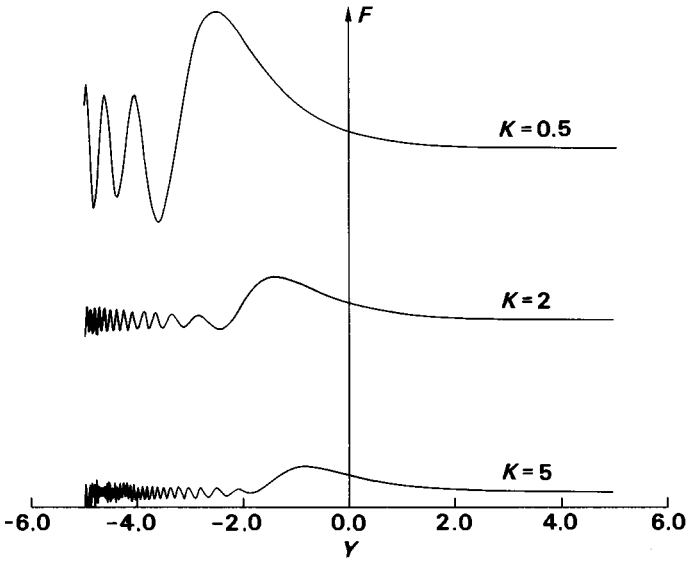

Figure 26. Logarithm of wave field normalized to value at the wall, for Bessel function solution, in the case of critical layer at the free stream, with plot extended below the wall, into the region of strong vorticity, approaching the essential singularity.

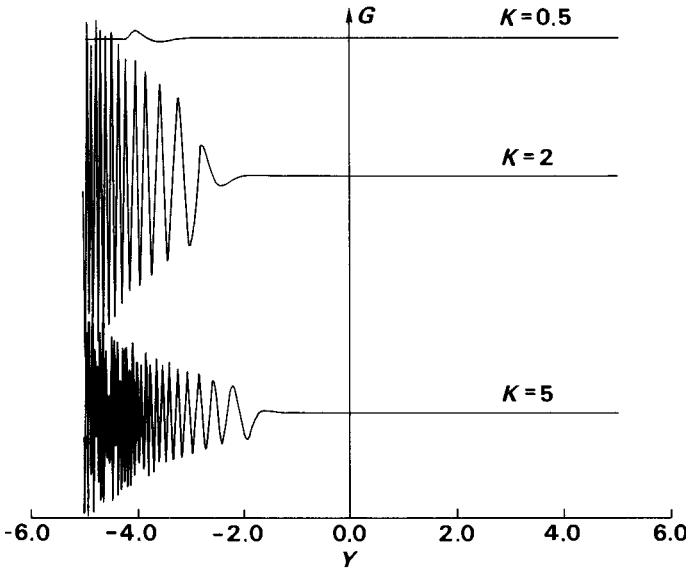

Figure 27. As figure 26, for a Neumann instead of a Bessel function.

region of interest, and it is an irregular singularity of the wave equation; the solution of the acoustic wave equation has an essential singularity for the phase, but only an algebraic one for the modulus. In a future paper the nature of the essential singularity for $\Omega \neq 1$, as a particular case of the extended hypergeometric equation is discussed. The present paper is concluded, with an illustration of the behaviour of the solution (8.17), in an extended region, up to five shear-layer thicknesses below the wall, to show the approach towards the essential singularity at $Y \to -\infty, \zeta \to \infty$.

The Bessel J and Neumann G functions are plotted separately, normalized to their value at the wall,

$$F(Y) \equiv \mathrm{e}^{-Y}\left\{\frac{J_{\sqrt{1+K^2}}(KM\mathrm{e}^{-Y})}{J_{\sqrt{1+K^2}}(KM)}\right\}, \tag{8.26}$$

$$G(Y) \equiv \mathrm{e}^{-Y}\left\{\frac{G_{\sqrt{1+K^2}}(KM\mathrm{e}^{-Y})}{G_{\sqrt{1+K^2}}(KM)}\right\}, \tag{8.27}$$

respectively, in figures 26 and 27, for five shear-layer thicknesses on either side of the wall (8.28 *a*):

$$-5 \leqslant Y \equiv y/L \leqslant +5, \tag{8.28 a}$$

$$K = 0.5, 2, 5, \tag{8.28 b}$$

and three dimensionless wavenumbers (8.28 *b*) and Mach number $n = 0.3$. In all cases the monotonic decaying waveform in the flow region changes to an oscillation below the wall; as the wavenumber increases, there are more oscillations per unit length and the amplitude decreases for F (figure 26) and increases for G (figure 27). The trend towards unbounded phase, as the essential singularity is approached, is apparent.

The authors acknowledge the benefit of the comments of the referees. Work was supported by project SNAAP of the EEC Aeronautics Research Programme.

References

Abramowitz, M. & Stegun, I. 1965 *Handbook of mathematical functions*. New York: Dover.

Almgren, M. 1976 Acoustic boundary layer influence on scale model simulation of sound propagation: theory and numerical examples. *J. Sound Vib.* **105**, 321–327.

Ballantine, S. 1927 On the propagation of sound in the general Bessel horn of infinite length. *J. Franklin Inst.* **203**, 85–101.

Bailey, W. M 1935 *The generalized hypergeometric function*. Cambridge University Press.

Balsa, T. F. 1976*a* The far-field of high-frequency convected singularities in sheared flows, with application to jet noise prediction. *J. Fluid Mech.* **74**, 193–208.

Balsa, T. F. 1976*b* Refraction and shielding of sound from a source in a jet. *J. Fluid Mech.* **76**, 443–456.

Bechert, D. & Pfizenmaier, F. 1975 On amplification of jet noise by pure tone excitation. *J. Sound Vib.* **43**, 581–592.

Blokhintsev, D. I. 1946 The propagation of sound in an inhomogeneous and moving medium. *J. Acoust. Soc. Am.* **18**, 322–341.

Booker, J. R. & Bretherton, F. P. 1966 A critical layer for internal gravity waves in a shear flow. *J. Fluid Mech.* **27**, 513–539.

Bretherton, F. P. 1967 Propagation in slowly varying waveguides. *Proc. R. Soc. Lond.* A **302**, 527–555.

Campos, L. M. B. C. 1978*a* The spectral broadening of sound by turbulent shear layers. I. Scattering by interfaces and refraction in turbulence. *J. Fluid Mech.* **89**, 723–749.

Campos, L. M. B. C. 1978*b* The spectral broadening of sound by turbulent shear layers. II. Broadening of experimental and aircraft noise. *J. Fluid Mech.* **89**, 751–779.

Campos, L. M. B. C. 1983*a* Sur la propagation du son dans les ecoulements non-uniformes et non-stationaires. *Rev. d'Acoust.* **67**, 217–233.

Campos, L. M. B. C. 1983*b* On magneto-acoustic-gravity waves standing or propagating vertically in an atmosphere. *J. Phys.* A **17**, 217–237.

Campos, L. M. B. C. 1983*c* On viscous and resistive dissipation of hydrodynamic and hydromagnetic waves in atmospheres. *J. Mech. Theor. Appl.* **2**, 861–891.

Campos, L. M. B. C. 1983*d* On three-dimensional acoustic-gravity waves in model anisothermal atmospheres. *Wave Motion* **5**, 1–14.

Campos, L. M. B. C. 1984 On the propagation of sound in nozzles of varying cross-section containing a low Mach number mean flow. *Z. Weltraumf.* **8**, 97–109.

Campos, L. M. B. C. 1985*a* On the fundamental acoustic mode in variable-area low Mach number nozzles. *Prog. Aerosp. Sci.* **22**, 1–27.

Campos, L. M. B. C. 1985*b* On vertical hydromagnetic waves in a compressible atmosphere under an oblique magnetic field. *Geophys. Astrophys. Fluid Dyn.* **32**, 217–272.

Campos, L. M. B. C. 1986*a* On waves in gases. I. Acoustics of jets, turbulence and ducts. *Rev. Mod. Phys.* **58**, 117–182.

Campos, L. M. B. C. 1986*b* On linear and nonlinear wave equations for the acoustics of high-speed potential flows. *J. Sound Vib.* **110**, 41–57.

Campos, L. M. B. C. 1987*a* On waves in gases. II. Interaction of sound with magnetic and internal modes. *Rev. Mod. Phys.* **59**, 363–462.

Campos, L. M. B. C. 1987*b* On longitudinal propagation in convergent and divergent nozzle flows. *J. Sound Vib.* **117**, 131–151.

Campos, L. M. B. C. 1988*a* On the properties of hydromagnetic waves in the vicinity of critical levels and transition layers. *Geophys. Astrophys. Fluid Dyn.* **40**, 93–132.

Campos, L. M. B. C. 1988*b* On oblique Alfvén waves in a viscous and resistive atmosphere. *J. Phys.* A **21**, 2911–2930.

Campos, L. M. B. C. 1988*c* On generalizations of the Doppler factor, local frequency, wave invariant and group velocity. *Wave Motion* **10**, 193–207.

Campos, L. M. B. C. 1990 On the dissipation of Alfvén waves in uniform and non-uniform magnetic fields. *Geophys. Astrophys. Fluid Dyn.* **48**, 193–215.

Campos, L. M. B. C. 1991 On cut-off frequencies for magneto-atmospheric waves. *Wave Motion* **15**, 103–119.

Campos, L. M. B. C. 1993*a* Exact and approximate methods for hydromagnetic waves in dissipative atmospheres. *Wave Motion* **17**, 101–112.

Campos, L. M. B. C. 1993*b* Comparison of exact solutions and the phase mixing approximation, for dissipative Alfvén waves. *Eur. Jl Mech.* B **12**, 187–216.

Campos, L. M. B. C. 1994 An exact solution for spherical Alfvén waves. *Eur. Jl Mech.* B **13**, 613–628.

Campos, L. M. B. C. 1998 Hydromagnetic waves in atmospheres with application to the Sun. *Theor. Comp. Fluid Dyn.* **10**, 37–70.

Campos, L. M. B. C. & Gil, P. J. S. 1995 On spiral coordinates with application to wave propagation. *J. Fluid Mech.* **301**, 153–173.

Campos, L. M. B. C. & Isaeva, N. L. 1992 On vertical, spinning Alfvén waves in a magnetic flux tube. *J. Plasma Phys.* **48**, 415–434.

Campos, L. M. B. C. & Lau, F. J. P. 1996*a* On sound in an inverse sinusoidal nozzle with a low Mach number mean flow. *J. Acoust. Soc. Am.* **100**, 355–363.

Campos, L. M. B. C. & Lau, F. J. P. 1996*b* On the acoustics of low Mach number bulged, throated and baffled nozzles. *J. Sound Vib.* **196**, 611–633.

Campos, L. M. B. C. & Saldanha, R. 1991 On oblique magnetohydrodynamic waves in an atmosphere under an oblique magnetic field of arbitrary direction. *Geophys. Astrophys. Fluid Dyn.* **56**, 237–251.

Drazin, P. G. &. Reid, W. H. 1981 *Hydrodynamic stability.* Cambridge University Press.

Eisenberg, N. A. & Kao, T. W. 1971 Propagation of sound in a variable area duct with a steady, compressible mean flow. *J. Acoust. Soc. Am.* **49**, 169–175.

Eltayeb, I. A. 1977 Linear wave motions in magnetic velocity shears. *Phil. Trans. R. Soc. Lond.* A **287**, 607–639.

Erdelyi, A. 1953 *Higher transcendental functions*. New York: McGraw-Hill.

Eversman, W. 1971 Effect of boundary layer on the transmission and attenuation of sound in an acoustically treated circular duct. *J. Acoust. Soc. Am.* **39**, 1372–1380.

Eversman, W. & Beckenmeyer, R. J. 1972 Transmission of sound in ducts with thin shear layers: convergence to the uniform flow case. *J. Acoust. Soc. Am.* **52**, 216–225.

Forsyth, A. R. 1902 *Theory of differential equations*. Cambridge University Press.

Forsyth, A. R. 1927 *Treatise of differential equations*. London: Macmillan.

Goldstein, M. E. 1979 Scattering and distortion of the unsteady motion on transversely sheared mean flows. *J. Fluid Mech.* **91**, 601–602.

Goldstein, M. E. 1982 High-frequency sound emission from moving point multipole sources embedded in an arbitrary transversely sheared mean flows. *J. Sound Vib.* **80**, 449–460.

Goldstein, M. E. & Rice, E. 1973 Effect of shear on duct wall impedance. *J. Sound Vib.* **30**, 79–84.

Graham, E. W. & Graham, B. B. 1968 Effect of a shear layer on plane waves in a fluid. *J. Acoust. Soc. Am.* **46**, 169–175.

Greenspan, H. P. 1968 *Theory of rotating fluids*. Cambridge University Press.

Hanson, D. B. 1984 Shielding of propfan cabin noise by the fuselage boundary layer. *J. Sound Vib.* **92**, 591–598.

Hersh, A. S. & Catton, I. 1971 Effects of shear flow on sound propagation in rectangular ducts. *J. Acoust. Soc. Am.* **50**, 992–1003.

Ho, C. M. & Kovaznay, L. S. G. 1976 Propagation of a coherent acoustic wave through a turbulent shear flow. *J. Acoust. Soc. Am.* **60**, 40–45.

Hughes, T. H. & Reid, W. H. 1965 On the stability of the asymptotic suction profile. *J. Fluid Mech.* **23**, 715–735.

Ince, E. L. 1926 *Differential equations*. New York: Dover.

Ishii, S. & Kakutani, T. 1987 Acoustic waves in parallel shear flows in a duct. *J. Sound Vib.* **113**, 127–139.

Jones, D. S. 1977 The scattering of sound by a simple shear layer. *Phil. Trans. R. Soc. Lond.* A **284**, 287–328.

Jones, D. S. 1978 Acoustics of a splitter plate. *J. Inst. Math. Appl.* **21**, 197–209.

Ko, S. H. 1972 Sound attenuation in acoustically lined circular ducts in the presence of uniform flow and shear flow. *J. Sound Vib.* **22**, 193–210.

Koutsoyannis, S. P. 1980 Characterization of acoustic disturbances in linearly sheared flows. *J. Sound Vib.* **68**, 187–202.

Koutsoyannis, S. P., Karamcheti, K. & Galant, D. C. 1980 Acoustic resonances and sound scattering by a shear layer. *Am. Aeron. Astron. Jl* **18**, 1446–1450.

Lighthill, M. J. 1953 On the energy scattered from interaction of turbulence with sound and shock waves. *Proc. Camb. Phil. Soc.* **44**, 531–548.

Lighthill, M. J. 1978 *Waves in fluids*. Cambridge University Press.

Lilley, G. M. 1973 On the noise from jets. *AGARD Conf. Proc.* **131**, 13.1–13.12.

Lin, C. C. 1955 *Theory of hydrodynamic stability*. Cambridge University Press.

Luke, Y. L. 1975 *Mathematical functions and approximations*. New York: McGraw-Hill.

Lyons, P. & Yanowitch, M. 1974 Vertical oscillations in a viscous and thermally conducting isothermal atmosphere. *J. Fluid Mech.* **66**, 273–288.

Mani, R. 1980 Sound propagation in parallel sheared flows in ducts: the mode estimation problem. *Proc. R. Soc. Lond.* A **371**, 393–412.

Mariano, S. 1971 Effect of wall shear layers on the sound attenuation in acoustically lined rectangular ducts. *J. Sound Vib.* **19**, 261–275.

PHILOSOPHICAL TRANSACTIONS OF THE ROYAL SOCIETY A MATHEMATICAL, PHYSICAL & ENGINEERING SCIENCES

McKenzie, J. F. 1973 On the existence of critical levels with application to hydromagnetic waves. *J. Fluid Mech.* **58**, 709–723.

McKenzie, J. F. 1979 Critical level behavior of ion-cyclotron waves. *J. Plasma Phys.* **22**, 361–376.

Miles, J. W. 1961 On the disturbed motion of a vortex sheet. *J. Fluid Mech.* **4**, 538–554.

Mohring, W., Muller, E. A. & Obermeier, F. 1983 Problems in flow acoustics. *Rev. Mod. Phys.* **55**, 707–724.

Moore, D. W. & Spiegel, E. A. 1964 Generation and propagation of waves in a compressible atmosphere. *Astrophys. Jl* **139**, 48–64.

Mungur, P. & Gladwell, G. M. L. 1969 Acoustic wave propagation in a sheared flow contained in a duct. *J. Sound Vib.* **9**, 28–48.

Mungur, P. & Plumblee, H. E. 1969 Propagation and attenuation of sound in a soft-walled annular duct containing a sheared flow. NASA SP-207, pp. 305–337.

Munt, R. M. 1977 Interaction of sound with a subsonic jet issuing from a semi-infinite jet-pipe. *J. Fluid Mech.* **83**, 609–620.

Myers, M. K. & Chuang, S. L. 1983 Uniform asymptotic approximations for duct acoustic modes in a thin boundary-layer flow. *Am. Inst. Aeron. Astron. Jl* **22**, 1234–1241.

Nayfeh, A. H., Kaiser, J. E. & Telionis, D. P. 1975 Acoustics of aircraft engine-duct systems. *Am. Inst. Aeron. Astron. Jl* **13**, 130–153.

Orr, W. M. F. 1907 The stability or instability of the steady motions of a perfect liquid and of a viscous liquid. *Proc. R. Ir. Acad.* A **27**, 9–68, 69–138.

Pridmore-Brown, D. C. 1958 Sound propagation in a fluid flowing through an attenuating duct. *J. Fluid Mech.* **4**, 393–406.

Rayleigh, J. W. S. 1880 On the stability, or instability, of certain fluid motions. *Proc. Lond. Math. Soc.* **11**, 57–70 (Papers **1**, 474–487).

Schlichting, H. 1933 Zur Enstehung der turbulenze bei der Plattenstromung. *Nachr. Ges. Wiss. Gott., Math-Phys. Klas.*, pp. 181–208.

Schlichting, H. 1951 *Boundary layer theory.* New York: McGraw-Hill.

Schmidt, D. W. & Tilmann, P. M. 1970 Experimental study of sound phase fluctuations caused by turbulent wakes. *J. Acoust. Soc. Am.* **47**, 1310–1324.

Scott, J. N. 1979 Propagation of sound waves through a linear shear layer. *Am. Inst. Aeron. Astron. Jl* **17**, 237–245.

Shankar, P. N. 1971 On acoustic refraction by duct shear layers. *J. Fluid Mech.* **47**, 81–91.

Shankar, P. N. 1972*a* Acoustic refraction and attenuation in cylindrical and annular ducts. *J. Sound Vib.* **22**, 233–246.

Shankar, P. N. 1972*b* Sound propagation in shear layers. *J. Sound Vib.* **40**, 51–76.

Sommerfeld, A. 1908 Ein betrag zur hydrodynamischen Erklaerung der turbulenten Fluessigkeitsbewegenger. *Proc. 4th Int. Congr. Math.* **3**, 116–124.

Swinbanks, M. A. 1975, The sound field generated by a source distribution in a long duct carrying sheared flow. *J. Sound Vib.* **40**, 51–76.

Tack, D. H. & Lambert, R. F. 1965 Influence of shear flow on sound attenuation in lined ducts. *J. Acoust. Soc. Am.* **38**, 655–666.

Tollmien, W. 1929 Ueber die Entstehung der Turbulenz. *Nachr. Ges. Wiss. Gott., Math-Phys. Klas.*, pp. 21–94.

Tsien, H. S. 1952 The transfer functions of rocket nozzles. *J. Am. Rocket Soc.* **22**, 139–143.

Turner, J. S. 1973 *Buoyancy effects in fluids.* Cambridge University Press.

Watson, G. N. 1944 *Bessel functions.* Cambridge University Press.

Whittaker, E. T. & Watson, G. N. 1927 *Course of modern analysis.* Cambridge University Press.

Yanowitch, M. 1967 Effect of viscosity on vertical oscillations of isothermal atmosphere. *Can. J. Phys.* **45**, 2003–2008.

PHILOSOPHICAL TRANSACTIONS OF THE ROYAL SOCIETY A MATHEMATICAL, PHYSICAL & ENGINEERING SCIENCES